



**EFFECT OF MALATHION ON THE  
MICROBIAL ECOLOGY OF ACTIVATED  
SLUDGE**

THESIS

Seth K. Martin, Senior Master Sergeant, USAF  
AFIT-ENV-MS-15-M-095

**DEPARTMENT OF THE AIR FORCE  
AIR UNIVERSITY**

***AIR FORCE INSTITUTE OF TECHNOLOGY***

**Wright-Patterson Air Force Base, Ohio**

DISTRIBUTION STATEMENT A  
APPROVED FOR PUBLIC RELEASE; DISTRIBUTION UNLIMITED.

The views expressed in this document are those of the author and do not reflect the official policy or position of the United States Air Force, the United States Department of Defense or the United States Government. This material is declared a work of the U.S. Government and is not subject to copyright protection in the United States.

AFIT-ENV-MS-15-M-095

EFFECT OF MALATHION ON THE MICROBIAL ECOLOGY OF ACTIVATED  
SLUDGE

THESIS

Presented to the Faculty  
Department of Engineering Physics  
Graduate School of Engineering and Management  
Air Force Institute of Technology  
Air University  
Air Education and Training Command  
in Partial Fulfillment of the Requirements for the  
Degree of Master of Science in Combating Weapons of Mass Destruction

Seth K. Martin, B.S.  
Senior Master Sergeant, USAF

27 March 2015

DISTRIBUTION STATEMENT A  
APPROVED FOR PUBLIC RELEASE; DISTRIBUTION UNLIMITED.

AFIT-ENV-MS-15-M-095

EFFECT OF MALATHION ON THE MICROBIAL ECOLOGY OF ACTIVATED  
SLUDGE

THESIS

Seth K. Martin, B.S.  
Senior Master Sergeant, USAF

Committee Membership:

Dr. W. F. Harper  
Chairman

LTC D. R. Lewis  
Member

Lt Col L. Racz  
Member

## Abstract

Decontamination activities may cause the release of contaminated washwater into the wastewater that eventually flows into a wastewater treatment facility. This raises concerns about the effect of chemical warfare agents (CWAs) on the microbial consortia that are responsible for cleaning the wastewater. This study investigated the impact of malathion on the microbial ecology of laboratory scale activated sludge communities. The Simpson Reciprocal Index decreased for three bioreactors operated in the absence of malathion, which showed that the microbial assemblage became less diverse during the course of the study. The species identified in the bioreactors belonged to well-known groups of heterotrophic and autotrophic bacteria, and these groups were represented in the presence and absence of malathion. *Nitrospira*, a key player in autotrophic nitrogen removal, decreased in relative abundance for the bioreactor exposed to  $0.1 \frac{mg}{L}$  of malathion but increased in the bioreactor exposed to  $3 \frac{mg}{L}$  of malathion, possibly due to interactions with heterotrophic groups that suffered inhibition. To the author's knowledge, this study is the first to document the ecological impacts of long term malathion exposure in bioreactors carrying out COD removal and nitrification.

AFIT-ENV-MS-15-M-095

*To my Wife and Daughters*

## Acknowledgements

I would like to express my sincere appreciation to a number of people whose encouragement, guidance, and efforts made this research effort possible. First, I am grateful to my research advisor, Dr. Willie Harper, for his research expertise and mentorship. Your guidance was motivating and insightful, enabling me to successfully complete a significant milestone. I would also like to recognize the exceptional support and instruction provided by Dr. Clarise Starr, Dr. James Baldwin and Dr. Wanda Lyons at the United States Air Force School of Aerospace Medicine Applied Technology and Genomics Center. Whenever I needed anything, whether it was time on an instrument, expertise for analyses, or identification of alternative methods, your assistance and technical support was always available and tailored to my needs and experience. Finally, I would like to thank my research partner, Captain Rauglas, and the lab technician, Kandace Bailey, for their dedicated efforts in keeping the reactors running smoothly throughout months of challenging schedules. It was a pleasure working alongside you and I gratefully acknowledge your contributions to my research.

Seth K. Martin

# Table of Contents

	Page
Abstract .....	v
Acknowledgements .....	vii
List of Figures .....	x
List of Tables .....	xi
I. Introduction .....	1
1.1 Motivation and Background .....	1
1.2 Research Objective .....	2
II. Literature Review .....	4
2.1 Organophosphates .....	4
2.2 Degradation .....	6
2.3 Waste Processing .....	7
2.4 Phylogenetic Analysis of Microbial Communities .....	9
2.5 Conclusion .....	10
III. Methodology .....	12
3.1 Laboratory Preparation .....	12
3.2 Sample Seed .....	13
3.3 COD and Nitrogen .....	16
3.4 DNA Extraction .....	16
3.5 Sample Quality .....	18
3.6 Sample Quantity .....	20
3.7 Sequencing Approach .....	22
3.8 Primer Preparation and Use .....	22
3.9 PCR .....	23
3.10 Gel Electrophoresis .....	26
3.11 Adapter and Barcode Ligation .....	30
3.12 Purification .....	30
3.13 Size Selection .....	31
3.14 Quality Control and Normalization .....	32
3.15 Emulsion PCR .....	35
3.16 ISP Quality Control and Enrichment .....	35
3.17 Sequencing .....	37
3.18 Bioinformatics .....	40



	Page
IV. Results and Analysis .....	42
4.1 Sequencing .....	42
4.2 Nitrification .....	44
4.3 Bioinformatics .....	49
4.4 Analysis .....	54
V. Conclusions .....	59
Bibliography .....	60

## List of Figures

Figure	Page
1	Reactor Diagram ..... 13
2	Contaminant Analysis ..... 19
3	Quantitation of Sample Nucleic Material ..... 21
4	16S rRNA Primer Alignment ..... 23
5	PCR Gradient Analysis ..... 25
6	Gel Electrophoresis ..... 29
7	Nucleic Acid Quantitation ..... 34
8	Reactor 1 Sequencing Data ..... 43
9	Reactor 2 Sequencing Data ..... 43
10	Reactor 3 Sequencing Data ..... 43
11	Reactor 1 Nitrogen, Suspended Solids, and pH ..... 46
12	Reactor 2 Nitrogen, Suspended Solids, and pH ..... 47
13	Reactor 3 Nitrogen, Suspended Solids, and pH ..... 48
14	Reactor 1 Phylogeny ..... 51
15	Reactor 2 Phylogeny ..... 52
16	Reactor 3 Phylogeny ..... 53

## List of Tables

Table	Page
1	PCR product concentrations (before malathion) ..... 20
2	Primer detail ..... 23
3	Gradient PCR Profile ..... 24
4	Sequencing Amplification Profile ..... 27
5	Sequencing Temperature Determination ..... 27
6	Region Table ..... 33
7	Sequencing Run Data ..... 42
8	Phylogenetic Analysis Results ..... 49
9	Increase after Acclimation ..... 55
10	Decrease after Acclimation ..... 55
11	Increase after Malathion ..... 55
12	Decrease after Malathion ..... 55

# EFFECT OF MALATHION ON THE MICROBIAL ECOLOGY OF ACTIVATED SLUDGE

## I. Introduction

### 1.1 Motivation and Background

Organophosphates (OPs) are widely used in the application of pesticides. Furthermore, some countries persist in maintaining chemical warfare stocks as insurance against neighboring states with similar capabilities or more technologically advanced conventional weapons. Non-state actors continue to explore weapons that generate publicity and differentiate their organization from others with more conventional capabilities. The public risk associated with exposure to OPs demands an adequate response to mitigate the hazard. This typically would involve a large quantity of water and a strong alkaline or chlorinated neutralizing agent, which would be collected and treated as hazardous waste or in a wastewater treatment facility.

Most municipal wastewater treatment plants in the United States use activated sludge systems. Activated sludge systems utilize a process that includes filtration, sedimentation and biodegradation to eliminate contaminants from an effluent stream. Early phases remove large debris through filtration. Secondary phases allow larger particulates to settle in a sedimentation tank. Bioremediation occurs in an aerobic reactor where activated sludge containing nitrifying bacteria and other microorganisms break down pollutants by feeding on oxidation products from compounds in the sludge. A final treatment stage removes contaminants using filtration before the treated effluent is released into the environment (1).

A diverse community of microbes develops using a suitable feedstock in the biodegradation phase to reduce or eliminate the contaminant. An aerobic sequencing batch reactor is an environment where the nitrogen cycle, a crucial process in the biosphere, is utilized to transform nitrogen compounds into energy sources for bacteria. Wastewater treatment plants take advantage of the nitrogen cycle and other transformation processes to biodegrade toxic substances into less harmful substances.

Recent studies indicate that the composition of the community may contribute to the effectiveness of its biodegradation capability with respect to OPs (2) (3). Further study is necessary to identify which genera are most able to survive in an OP environment and whether specific genera or combinations may be more effective at biodegradation. Various methods exist for the evaluation of bacterial communities. In recent years, the development of next generation sequencing technology has extended the breadth and depth of evaluation results. The application of sequencing technology offers further phylogenetic detail that may improve bioremediation research efforts. Bioremediation offers an economical and efficient means to treat water supplies and developing optimal parameters ensures effective elimination of OP contaminants.

## **1.2 Research Objective**

This research project inquires: What is the impact of malathion to bacterial consortia in activated sludge systems? Which bacteria are most impacted by the presence of malathion? What traits are displayed by bacteria that exist in environments contaminated with malathion? The objectives for the research are assess the diversity of the bacterial community and determine any effects on the community structure.

In order to simulate the environment where an OP may be introduced into a wastewater treatment plant, it was necessary to build three bench-scale activated sludge sequencing batch reactors. The setup consisted of three containment vessels

with 2.0 L capacity, each with different concentrations of substrate. The three reactors were seeded with activated sludge from a local wastewater treatment plant and the sludge was provided with simulated wastewater containing macro and micro nutrients. Malathion, a commonly used, commercially available, and less toxic OP pesticide was used as a surrogate for higher toxicity nerve agents. After a period of acclimation to the laboratory environment, malathion was added to the influent and pumped into two of the reactors continuously for 30 days maintaining reactor substrate concentrations of  $0.1 \frac{mg}{L}$  and  $3 \frac{mg}{L}$ .

The study evaluated the ecology of bacteria when exposed to OPs. Genomic DNA from biomass samples was extracted using procedures adopted from Janeczko (1). The MoBio PowerSoil DNA isolation kit was used to extract nucleic material from bacterial samples for PCR analysis and genetic identification. The three reactors were evaluated using genetic sequencing over an extended period prior to malathion exposure to establish a baseline phylogeny and identify community changes due to the transition to a laboratory environment. Additional samples were taken after exposure for a period of one month and sequenced using next generation sequencing.

## II. Literature Review

### 2.1 Organophosphates

Organophosphates have long been used in applications as pesticides and military nerve agents. The toxicity of OPs is well-known and contributed to their historical development as weapons of mass destruction in the inventories of Nazi Germany, Soviet Russia and the United States (4). Common examples of pesticides are malathion, parathion, and diazinon. Perhaps more well-known are the notorious chemical nerve agents VX, sarin, soman, and tabun. The toxicity of OPs varies with exposure and the species of OP encountered. Poisoning cases associated with OPs occur worldwide and are frequently associated with suicides in agrarian locations (5). An epidemic poisoning occurred in Pakistan where 7,500 workers were exposed to malathion, an OP insecticide. At its peak, it is estimated that 2,800 workers were casualties and at least five died from the effects (6). Malathion degrades to more toxic products such as malaoxon and isomalathion. Malaoxon is an oxidative metabolite that is 61 times more toxic than malathion. Isomalathion is 1000 times more toxic (7). However, mammals and birds have higher carboxylesterase activity than pests such as insects, allowing malathion removal at lower concentrations and preventing more toxic metabolites from accumulating (8).

Early research into OP chemistry and use began in the 1800s with French organic chemist P. Clermont synthesizing the first cholinesterase inhibitor, TEPP. In 1932, a German chemist first described nervous systems effects including a choking sensation and dimming of vision. Another German chemist, G. Schrader, studied OPs in hopes of producing new insecticides, but later became known as “the father of nerve agents” for his accidental discovery of both sarin and tabun. The Nazi government seized on his discovery, placing him in charge of a chemical warfare agent program

that produced large quantities of OPs called G-agents. Another series of chemical agents, the V-agents, was first produced by the British during World War II. After the war, American companies used Schrader's research to produce pesticides including malathion, parathion and azinphosmethyl. OP use as a pesticide was boosted later when organochlorine pesticides were banned in the 1970s (9).

Organophosphates are esters of phosphoric acid with applications as pesticides and are characterized by their chemical structural features. These include a terminal oxygen connected to a phosphorus by a double bond. The phosphorus is bonded to two lipophilic groups and a leaving group, which is often a halide. Examples of this type of OP are the nerve agents VX and sarin. Some compounds replace the double-bonded oxygen with a terminal sulfur. Pesticides such as parathion and malathion have this feature. In mammals, metabolism removes a lipophilic group, resulting in toxic effects less severe than that of nerve agents. In insects, metabolism involves oxidation of the compound, replacing the sulfur with a terminal oxygen improving its enzyme inhibition capability (9).

However, both groups function in a similar manner. In the human body, OPs enter through dermal, inhalation, or ingestion routes and are distributed throughout the body. When OPs reach the nervous system, they have significant toxic effects. OPs inhibit acetylcholinesterase (AChE), an enzyme. Inhibition is caused by phosphorylation of the serine hydroxyl residue, inactivating AChE. This leads to the accumulation of acetylcholine (ACh) at postsynaptic membranes. In early stages, the phosphorylation may be reversible, but eventually aging occurs resulting in permanent covalent bonds. Excess ACh causes permanent stimulation at cholinergic nerve junctions and in the muscles. Symptoms may progress from parasympathetic and sympathetic hyperactivity to lethal effects when OPs are present in sufficient concentration (9).



## 2.2 Degradation

Numerous studies have documented various means for the biodegradation of pesticides and chemical warfare agents. Insecticides generally fall within one of three categories of organophosphates: phosphotriesters, thiophosphatetriesters, or phosphorothioesters. The primary difference between each is the number of oxygen or sulfur groups attached to the phosphorus center. In the case of malathion, a phosphorothioester, the phosphorus center is double bonded to a sulfur, with an opposing sulfur leaving group bonded to the phosphorus center (10). These varying structures play a role in the effectiveness of microorganisms' mechanisms to utilize the constituent chemical bonds to satisfy energy and nutrition requirements.

The primary tool that bacteria and other microorganisms use is enzymes. Enzymatic hydrolysis generally occurs using a multistep processes involving phosphatase, esterase, hydrolase and oxygenase (11). Some enzymes have broad substrate specificity, such as organophosphate hydrolase (OPH), which is used by bacteria like *Pseudomonas diminuta* (12). OPH has shown the capability to degrade a wide variety of OPs into less toxic end products. It has also been shown to be an effective enzyme in degrading the highly toxic VX nerve agent, along with other phosphate-sulfur bond OPs such as demeton, malathion, acephate, and phosalone (13) (14). Often, one or more enzymes is required and may produce varying levels of results depending on the substrate involved. Another widely studied enzyme is organophosphorus acid anhydrolase (OPAA), isolated from *Alteromonas*. OPAA works well at hydrolyzing phosphorus-fluorine bonds, but works slowly against phosphorus bonds with oxygen and doesn't work against sulfur (15).

Several species of soil bacteria including *Bacillus*, *Pseudomonas*, *Flavobacterium*, *Arthrobacter*, *Micrococcus* and others have shown varying capability to degrade OPs through species-unique enzymatic processes (16). *Bacillus* shows significant phos-

phatase activity, particularly at higher pH levels ( $\sim 8.0$ ) (17). *Pseudomonas sp.* are frequently named as a successful genera capable of degrading malathion using enzymatic hydrolysis via dicarboxylesterase or carboxylesterase (18). Degradation by *Rhizobium sp.* has also been reported implicating carboxylesterase as the likely pathway (19). Some organisms require additional carbon sources in cometabolism processes to successfully degrade organophosphorous compounds. Sodium succinate and sodium acetate are examples of cometabolism compounds that enhance malathion degradation by *Acinetobacter johnsonii* MA19 (20). Furthermore, a genetic basis for OP degradation has been established. Organophosphorous degrading bacteria have been genetically engineered with genes that express enzymatic capability and proven successful. In one example of genetically engineered bacteria, *Pseudomona putida* was isolated from p-nitrophenol contaminated waste and engineered to degrade OP compounds simultaneously with p-nitrophenol (21). Additionally, there is some evidence to suggest plasmid involvement during malathion degradation in *Micrococcus sp.* (12).

## 2.3 Waste Processing

Wastewater treatment involves a series of filtering, sedimentation, and treatment processes that prevent undesirable substances from reemerging in water supplies for human consumption. Initially, wastewater passes through screens that remove large debris. It then flows to a settling tank where solid particles are allowed to precipitate and the fluid portion is separated from it. The fluid is aerated and a nitrifying bacterial community develops in the nutrient-rich, oxidation tank. At this point, the mixture is called activated sludge.

Activated sludge consists of a wide variety of microorganisms. One group of bacteria involved in the biodegradation process is the nitrifying bacteria. Nitrify-

ing bacteria oxidize inorganic nitrogen compounds for energy consumption. These can be further subdivided into ammonia oxidizers and nitrite oxidizers. Ammonia oxidizers, including members from Proteobacteria, are represented by genera *Nitrosomonas*, *Nitrospira*, *Nitrosolobus*, and *Nitrosovibrio* (beta-class) and *Nitrosococcus* (gamma-class). The nitrite oxidizers are also members of Proteobacteria, including genera *Nitrobacter* (alpha-class), *Nitrococcus* and *Nitrospina* (both gamma-class). *Nitrospira* (*Nitrospira* phylum) is also a nitrite oxidizer. The ammonia oxidizers are lithotrophic bacteria that oxidize ammonia into nitrite through the enzyme ammonia monooxygenase (AMO), and then the nitrite oxidizers oxidize the nitrite into nitrate using the enzyme nitrite-oxidoreductase (NO<sub>2</sub>-OR) (17).

The microorganisms are fed a mixture of nutrients and begin consuming dissolved compounds in the solution. After a certain period of time, the sludge settles to the bottom where it may be recycled for use again, disposed in effluent wastewater streams, or sent to a waste processing area for disposal at a landfill or as fertilizer. The amount of time spent in the activated sludge phase affects the removal rate of contaminants. The contaminant removal capacity of the activated sludge is dependent on factors such as the microorganism community structure and performance. Additionally, since the activated sludge is a biomass, the contaminant profile and concentration of its constituents will affect the ability of living organisms exposed to it to perform their intended functions (1). Understanding the effects of OP contaminants and the ability of a wastewater treatment facility to effectively eliminate their toxicity is a key component of the final phase of recovery. Once waste leaves the facility, it will be reintroduced to the environment where it may once again present potential exposure risk.

## 2.4 Phylogenetic Analysis of Microbial Communities

Microbial detection and community structure phylogeny are determined using various methods. Bergey's Manual of Determinative Bacteriology provides a flow chart method for identification and comparison of observed sample culture characteristics with known bacterial characteristics. Bergey's Manual was used to identify the *Pseudomonas* genus during an evaluation of malathion degradation during continuous cultivation in diluted and undiluted nutrient broths (16). This analytical approach involves morphological and cultural means to identify the organism's physiology.

In the last few decades, molecular techniques that amplify nucleic material using polymerase chain reaction (PCR) have become more common and specific. The replication process for PCR involves heating and denaturing the DNA to unwind the double helix and separate the two sugar-phosphate backbones by disassociating the hydrogen bonds between the nucleotide base pairs. The reaction then cools during the annealing step, which allows a forward and reverse primer to attach and bind to the target region at primer-specific temperatures. The reaction continues with a rise to the optimal polymerase temperature so that the enzyme can synthesize and elongate the new DNA strand with deoxynucleotide triphosphate (dNTPs) bases that have been added to the reaction. The goal of PCR is to produce exponentially greater quantities of the target region, so the cycle is repeated several times.

The PCR process was further improved and evaluated using DNA sequencing. DNA sequencing is the process of analyzing DNA strands to determine the order of the constituent nucleotides. In this study, a relatively new technology called massively parallel, or next generation sequencing (NGS), is used to evaluate samples for bacterial community structure. Massively parallel sequencing is possibly more descriptive, alluding to the computing power required to identify nucleotide bases real-time during PCR. All NGS instruments include: random fragmentation and ligation with a custom

library, amplification on a bead or glass, direct detection during sequencing, millions of reactions during a run, shorter reads than capillary sequencers, and digital, paired-end (from both ends) reads for more accurate, mapped quantitative analysis (22).

The 16S ribosomal ribonucleic and deoxyribonucleic acid gene sequencing analysis method is one of the more common methods of analyzing bacterial phylogeny. The 16S gene is present in almost all bacteria and has been conserved over time (23). It is also specific enough for even rare isolates due to its ubiquitous presence, size and functional purpose (24). Alternative quantitative techniques are also available, such as automated ribosomal intergenic spacer analysis (ARISA), which provided a community profile as an exploratory tool in the case of *Candidatus Accumulibacter* (25). The 16S method is used in this study.

## 2.5 Conclusion

In summary, organophosphates have existed for many years, but only in the last two centuries have their chemical properties and toxic effects become well-known. The study of OPs has led to the creation of military nerve agents and pesticides that are still in use. Organophosphates bind to ACh enzymes and cause overstimulation at the post-synaptic junctions between the nervous system and muscles. Overstimulation may be fatal. When OP hazardous materials incidents or terrorist attacks occur, the response will likely involve decontamination and disposal. Disposal at wastewater treatment facilities is an economical and possibly unavoidable consequence.

Most municipal wastewater treatment plants in the United States use activated sludge systems. Activated sludge systems utilize a process that includes filtration, sedimentation and biodegradation to eliminate contaminants from an effluent stream. A diverse community of microbes develops using a suitable feedstock in the biodegradation phase to reduce or eliminate the contaminant. Recent studies indicate that the

composition of the community may contribute to the effectiveness of its biodegradation capability with respect to OPs. This community may be characterized in greater detail using the recently developed sequencing technologies.

### III. Methodology

#### 3.1 Laboratory Preparation

An initial assessment of laboratory conditions and resources was conducted one month prior to obtaining the sample from the water treatment plant. An initial inventory of equipment included a 2 L bench-scale sequencing batch reactor, peristaltic pumps and associated hoses and tubing, gas and liquid solenoids, electronically-controlled switches, laptops with control software, liquid reservoir and containment trays, and associated mounting hardware. Each equipment item was inspected for cleanliness and operational condition. A cleaning solution consisting of Alconox and deionized water was used to clean the tubing and reactors and then rinsed with deionized water until all remaining residue was removed. All reactor pumps and lengths of tubing were calibrated using 15 runs of deionized water to verify volumetric throughput.

The three continuously operated benchtop reactors were assembled (Fig. 1). An influent water tank and two feed solutions (described below) in 1 L (A) and 0.5 L (B) glass containers with plastic screw-on lids were connected via tubing through a peristaltic pump to each of the three reactors. A glass tube extending from each of the reactor lids to the liquid surface was connected via tubing through an electric solenoid valve to the effluent tank. Compressed air at 1–3 psi was pumped into each tank via tubing through an electric solenoid valve. Filtered air in and air out were also connected to each tank via tubing and controlled with an electric solenoid valve. Control of all pumps and switches was maintained using a laptop and a software-controlled timing switch. Each of the reactors were isolated from the others with no transference of air or liquid between them.

A feed solution was prepared using methods adopted from previous studies in

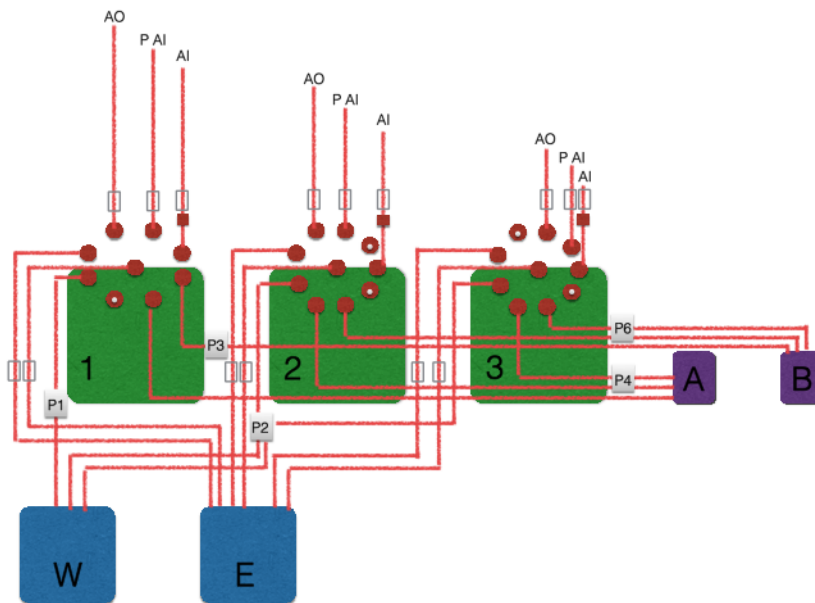


**Figure 1. Reactor Diagram**

the lab (1). Stock solutions were prepared as follows. Feed A consisted of 89.2 g  $\text{NaHCO}_3$  and 2 L of deionized water. Feed B consisted of 2.5 g  $\text{C}_2\text{H}_3\text{NaO}_2$ , 12.0 g Peptone, 4.52 g  $\text{NH}_4\text{Cl}$ , 13.72 g  $\text{MgCl}_2 \bullet 6\text{H}_2\text{O}$ , 3.44 g  $\text{CaCl}_2 \bullet 2\text{H}_2\text{O}$ , 1.335 g  $\text{KH}_2\text{PO}_4$ , 40 mL trace element solution and 2 L deionized water. The trace element solution consisted of 2.73 g  $\text{C}_6\text{H}_8\text{O}_7$ , 2.00 g  $\text{C}_9\text{H}_9\text{NO}_3$ , 0.36 g  $\text{C}_6\text{H}_6\text{NNa}_3\text{O}_6 \bullet 2\text{H}_2\text{O}$ , 0.15 g  $\text{C}_{10}\text{H}_{13}\text{N}_2\text{Na}_3\text{O}_8 \bullet 4\text{H}_2\text{O}$ , 1.50 g  $\text{FeCl}_3 \bullet 6\text{H}_2\text{O}$ , 0.25 g  $\text{H}_3\text{BO}_3$ , 0.15 g  $\text{ZnSO}_4 \bullet 7\text{H}_2\text{O}$ , 0.12 g  $\text{MnCl}_2 \bullet 4\text{H}_2\text{O}$ , 0.07 g  $\text{CuSO}_4 \bullet 5\text{H}_2\text{O}$ , 0.03 g  $\text{KI}$ , 0.03 g  $\text{Na}_2\text{MoO}_4 \bullet 2\text{H}_2\text{O}$ , 0.03 g  $\text{CoCl}_2 \bullet 6\text{H}_2\text{O}$ , 0.03 g  $\text{NiCl}_2 \bullet 6\text{H}_2\text{O}$ , 0.03 g  $\text{Na}_2\text{WO}_4 \bullet 2\text{H}_2\text{O}$ , and 1 L of deionized water. All three stock solutions were stored in a laboratory refrigerator and dispensed as needed into autoclaved glass containers for use.

### 3.2 Sample Seed

The activated sludge was obtained from Fairborn, Ohio Water Treatment Facility on Day 1. A 4 L sample was removed from an oxidation tank and funneled into a



glass screw-top container. Heavy seasonal precipitation contributed to higher than normal dilution of the sample. The 4 L sample was transported to the laboratory and allowed to settle. 2 L of water was decanted from the sample and the remaining 2 L of activated sludge was poured into Reactor 1. A manual feed was initiated using Feed A and Feed B followed by the start of an automated cycle.

The automated cycle covering 12 hrs was controlled using a software program, electronically controlled switches and solenoids and operated continuously. It consisted of aeration, settling, effluent purge, influent deionized water and feed solution addition. During the 10:50 hr aeration period, filtered compressed air was pumped into the reactors at constant pressure to maintain approximately  $7 \frac{mg}{L}$  concentration dissolved oxygen (DO) in the mixed liquor. Air was vented out during the aeration period, except during the effluent purge, which occurred 5:30 hrs into the cycle, pausing aeration for 4 sec. During the last second, the 35.9 mL of effluent was purged. At the end of 10:50 hr aeration period, the mixed liquor was allowed to settle for 1 hr. After settling, a purge air line was switched on and the supernatant effluent was pumped for 45 sec from the tanks into a graduated cylinder. Then, 624 mL of deionized water, 36.0 mL of Feed B, and 8.0 mL of Feed A were added to the tank, finishing at the end of the 12 hr cycle. Reactors 2 and 3 received 627 mL of deionized water and 38.2 mL of Feed B during operation due to measured delivery differences noted during calibration. Two full cycles occurred each day for the reactors during the operational period.

Reactor 1 activated sludge stabilization and adaptation to the synthetic influent continued for 60 days. The wasted mixed liquor purge solution was collected and added to Reactors 2 and 3 on Day 70 of operation. Air pressure and liquid volumes were calibrated and adjusted to account for unique flow rates associated with each reactor and associated lengths of tubing. All three reactors were operated continuously

at room temperature. The reactor vessels were maintained using brushes and deionized water to remove biomass material from the sides of the vessel. Hoses and tubing were periodically inspected and cleaned to ensure a consistent flow rate. A Mettler Toledo FiveEasy bench top pH meter was also used to electrometrically determine the pH of the mixed liquor solutions. The bench top meter was used as described in Standard Method 9040C, pH (Electrometric) (26).

After Reactor 1 had operated for 250 days and all three reactors had stabilized using the synthetic influent feed solution, malathion was added to the influent feed for Reactors 1 and 3. Reactor 1 received malathion-spiked influent at a rate sufficient to maintain  $0.1 \frac{mg}{L}$  concentration and Reactor 3 received at a rate to maintain  $3 \frac{mg}{L}$ . Reactor 2 did not receive malathion and was maintained as the control. The influent water volume was 624 mL per cycle.

$$Conc, Malathion, R1, \frac{mg}{L} = \frac{(0.1 \frac{mg}{L})(2L)}{0.624L} = 0.3205 \quad (1)$$

$$Vol, Malathion, R1, mL = \frac{(0.3205 \frac{mg}{L})(4L)}{100 \frac{mg}{L}} = 0.01282L(\frac{1000mL}{1L}) = 12.82 \quad (2)$$

$$Conc, Malathion, R3, \frac{mg}{L} = \frac{(3 \frac{mg}{L})(2L)}{0.624L} = 9.615 \quad (3)$$

$$Vol, Malathion, R3, mL = \frac{(9.615 \frac{mg}{L})(4L)}{100 \frac{mg}{L}} = 0.3846L(\frac{1000mL}{1L}) = 384.6 \quad (4)$$

$$Vol, 0.1 \frac{mg}{L} > 3 \frac{mg}{L} Malathion, R3, mL = \frac{(3 \frac{mg}{L})(2L)}{100 \frac{mg}{L}} = 0.06L(\frac{1000mL}{1L}) = 60 \quad (5)$$

### 3.3 COD and Nitrogen

Chemical Oxygen Demand (COD), Nitrogen-Ammonia ( $\text{NH}_4\text{-N}$ ), Nitrogen-Nitrate ( $\text{NO}_3\text{-N}$ ), and Nitrite ( $\text{NO}_2^-$ ) were evaluated using Standard Methods 8000, 10031, 10020, 8153 (27), respectively, and procedures adopted from Janeczko (1). For each method, a calibration curve consisting of five measurements at known concentrations was generated with linear regression and interpolation.

Thirteen each COD digestion vials,  $\text{NH}_4\text{-N}$  vials,  $\text{NO}_3\text{-N}$  vials, and 10 mL test tubes for  $\text{NO}_2^-$  tests were obtained and labeled for three effluent tests and one mixed liquor test per reactor, plus one additional tube as a negative control for all three reactors. Effluent and mixed liquor samples were obtained from the gravimetric analysis filtrate. An Agilent Cary 60 UV-Vis Spectrophotometer was used to measure absorbance for each reaction. The absorbance from the samples was identified on the calibration curve and the associated concentration recorded.  $\text{NO}_3\text{-N}$  effluent had a dilution of 2. All others were calculated with a dilution of 1. A single mixed liquor value and mean effluent value for the three COD,  $\text{NH}_4\text{-N}$ ,  $\text{NO}_3\text{-N}$ , and  $\text{NO}_2^-$  tests for each reactor was obtained.

### 3.4 DNA Extraction

DNA was extracted using the Mo Bio Laboratories, Inc. PowerSoil® DNA extraction kit and protocol (28) and procedures adopted from Janeczko (1). Nine 2 mL collection tubes, 1 PowerBead Tube, and 1 Spin Filter Tube were obtained for each of the three reactors, labeled, and placed in a microcentrifuge tube rack. A 1 mL sample was obtained from the unfiltered 25 mL mixed liquor sample and centrifuged at  $10,000 \times g$  for 2 min to pellet the bacteria. The liquid supernatant was then removed and discarded. The buffer solution from the PowerBead Tubes was then added to the bacteria pellet and vortexed briefly to resuspend the pellet in solution. The

mixed buffer and pellet were then added back to the PowerBead tube. 60  $\mu\text{L}$  of Mo Bio proprietary disruption agents was added to promote cell lysis and the tube was vortexed briefly. Each tube was then secured horizontally to the vortex pad with tape and vortexed for 10 min for homogenization and cell lysis.

The tube was then centrifuged at 10,000 x g for 30 sec and the supernatant transferred to a clean collection tube. 250  $\mu\text{L}$  of inhibitor removal reagents was added to precipitate contaminants and vortexed for 5 sec and then incubated at 4°C for 5 min. The tube was then centrifuged at 10,000 x g for 1 min and the supernatant transferred to a clean collection tube. 200  $\mu\text{L}$  of additional inhibitor removal reagents was added for further sample purification and vortexed for 5 sec and then incubated at 4°C for 5 min. 750  $\mu\text{L}$  of supernatant was transferred to a clean collection tube and 1200  $\mu\text{L}$  of vortexed high concentration salt solution was added. The tube was then vortexed for 5 sec. 675  $\mu\text{L}$  of the solution was transferred onto a spin filter with a silica membrane and centrifuged at 10,000 x g for 1 min. The flow through was discarded and the filter transferred to a clean collection tube.

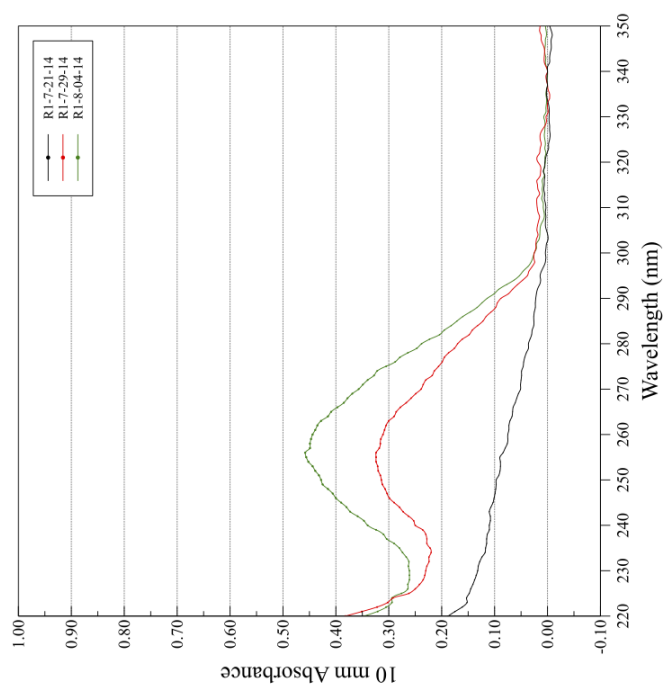
The spin filter was loaded, centrifuged, and transferred two additional times with the remaining solution for a total of 3 sample loads. 500  $\mu\text{L}$  of ethanol-based wash solution was added to the spin filter and centrifuged at 10,000 x g for 30 sec. The flow through was discarded and the filter transferred to a clean collection tube. The spin filter was centrifuged at 10,000 x g for 1 min to remove all residual wash solution and transferred to a clean collection tube. 100  $\mu\text{L}$  of sterile elution buffer was added and centrifuged at 10,000 x g for 30 sec. The spin filter was removed and the extracted sample placed in -80°C storage.

### 3.5 Sample Quality

The extracted samples were evaluated for contamination using a Nanodrop<sup>TM</sup> 1000. The instrument was cleaned with deionized water prior to use. A blanking buffer of deionized water was used as a reference. A 2  $\mu$ L drop from each sample was pipetted onto the measurement pedestal and the sampling arm was lowered to a 10 mm path length. A measurement was taken for each sample and the pedestal cleaned with a lab tissue afterwards. Each measurement was reviewed, saved, and exported. The A260/A280 and A260/A230 ratios were examined for appropriate values.

Contaminants from reagents used in sample DNA extraction may be identified by shifts in the spectra at the A260 peak, A230 trough, and A280 value. Examples of contaminants include: TRIzol, phenol, guanidine HCL, and guanidinium isocyanate. Low A260/A230 ratios may indicate residual phenols, guanidine, or glycogen. High A260/A230 ratios may indicate inappropriate blank measurements. Low A260/A280 ratios may indicate residual reagent contamination, such as phenols. The generally accepted value for pure DNA is 1.8 for A260/A280 and slightly higher values in the range of 2.0 - 2.2 for A260/A230 (29).

Three samples were selected from Reactor 1 on Days 105, 112, and 119 of operation (Fig. 2). The A260/A280 values for all three samples ranged between 1.83 and 2.07. The A260/A230 values ranged between 0.57 and 1.7. However, the low A260/A230 values were likely affected by low concentrations of dsDNA in the samples and the proximity to the lower limits of detection. The detection limits for the Nanodrop<sup>TM</sup> 1000 are 2 ng/ $\mu$ L to 75 ng/ $\mu$ L at the 10mm pathlength (30). This purity values at the A260/A280 levels and the location of the peaks were within the proper ranges. High purity DNA was obtained using the previously described DNA extraction methods and suitable for downstream processing.



Module: Nucleic Acid  
Path: 10 mm

Sample ID	ng/ul	A230	A260	A280	340 raw	260/280	260/230
R1-7-21-14	3.74	0.132	0.075	0.036	0.044	2.07	0.57
R1-7-29-14	15.56	0.23	0.311	0.17	-0.006	1.83	1.35
R1-8-04-14	22.2	0.261	0.444	0.238	-0.004	1.87	1.7

Figure 2. Contaminant Analysis

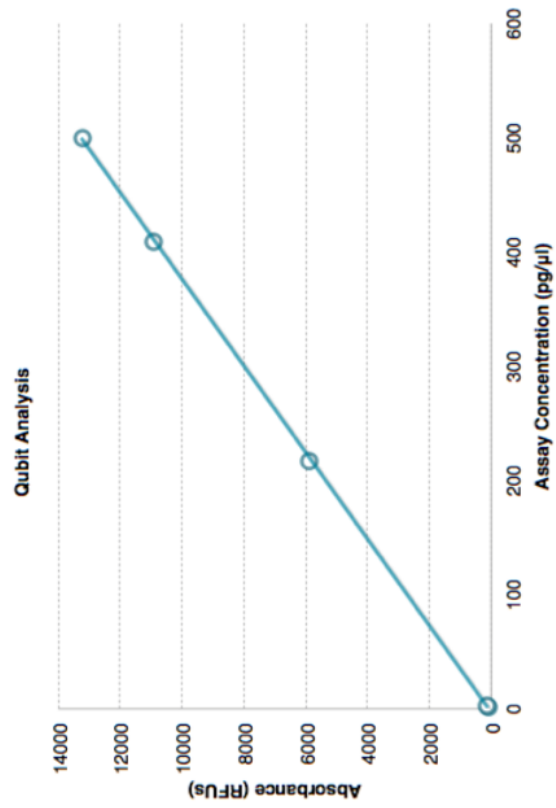
### 3.6 Sample Quantity

**Table 1. PCR product concentrations (before malathion)**

Primer Set	Reactor 1 (ng/ $\mu$ L) Min, Max, Mean	Reactor 2 (ng/ $\mu$ L) Min, Max, Mean	Reactor 3 (ng/ $\mu$ L) Min, Max, Mean
BacU_EX_11 / BacU_EX_E786F	8.070, 72.7, 43.55	1.040, 68, 34.37	0.887, 49.3, 27.38
Bac-U1_13 / BacU_UX_U1053F	31.50, 69.3, 50.91	15.7, 63.1, 45.67	14.1, 70, 39.17
805r / Bact_U2_15	1.10, 84, 26.65	3.37, 175, 58.67	4.94, 169, 65.55

The reactor samples were evaluated for initial quantity using the Qubit<sup>®</sup> 2.0 fluorometer and a dsDNA HS (High Sensitivity) Assay Kit. Two thin-wall, clear 0.5 mL PCR tubes were labelled and filled with 189  $\mu$ L of Qubit<sup>™</sup> working solution and 1  $\mu$ L of Qubit<sup>™</sup> dsDNA HS reagent. 10  $\mu$ L of 0 ng/ $\mu$ L Standard #1 was added to one tube and 10  $\mu$ L of 10 ng/ $\mu$ L Standard #2 was added to the other. Both were allowed to incubate at room temperature for 2 min and then measured to calibrate the instrument. 194  $\mu$ L of working solution, 1  $\mu$ L of dsDNA HS reagent, and 5  $\mu$ L of each sample were added to 0.5 mL PCR tubes and incubated at room temperature for 2 min. Each was then measured, noted, and the data exported to a file.

The fluorometer uses dyes that are selective and only bind to DNA, minimizing the effect of contaminants on the quantitative measurement (31). The three DNA samples selected for analysis before PCR ranged between 0.133 and 16.36 ng/ $\mu$ L (Fig. 3). The measurement was repeated after PCR using the initial primers without barcodes and adapters (Tab. 1). For the medium quantity assay (Day 113), there was a 29 - 77 times increase in nucleic material. The largest quantity assay (Day 119) increased by 9 - 30 times.



Assay	Assay Conc (pg/ul)	Absorbance (RFUs)	Sample Conc (ng/ul)
Std 1	1	68.23	0.04
Assay 21 Jul	3.33	153.27	0.133
Assay 27 Jul	217	5901.81	8.68
Assay 4 Aug	409	10898.55	16.36
Std 2	500	13199.5	20

Figure 3. Quantitation of Sample Nucleic Material



### 3.7 Sequencing Approach

The overall objective was to conduct six total sequencing iterations representing samples from each of the three reactors prior to malathion exposure and after exposure. Broad coverage of the 16S ribosomal gene was also a consideration. A multiplex approach using fragment lengths of 350 - 500bp was selected initially. Multiplex sequencing was attempted on the first sequencing run, but later runs were conducted using a single primer pair. Early evaluation of primer performance and use was accomplished using primers with manually ligated sequencing adapters and barcodes. The follow-on evaluation of samples from before and after malathion exposure was conducted using fusion primers with sequencing primers and barcodes attached. The barcoding methodology highlighted evolution of the bacterial community. Barcode 1 represented the initial period of operation during the first 90 days. Barcodes 2 and 3 represented the early and late periods, respectively, of the acclimation period prior to malathion exposure on Day 250. Barcode 5 represented the 30 days of malathion exposure. Due to sampling constraints, Barcode 4 was eliminated from the final evaluation.

### 3.8 Primer Preparation and Use

A variety of primers were surveyed for use during sequencing. Primers were selected from known high coverage rate pairs from previous research (32) (33) (34) (35) (36). An example bacteria, *Escherichia coli*, NC\_011745.1, was examined using a BLAST search (37). The 16S ribosomal rRNA gene, ECED1\_16S\_1 [3868436..3870438], was located and downloaded using the graphical interface. The sequence was used to conduct a BLAST search versus the list in FASTA format.

The offsets and strandedness were associated and mapped on a linear scale representing the 16S ribosomal rRNA gene (Fig. 4). Primer pairs were reviewed using the

**Table 2. Primer detail**

Sequence (5' to 3')	Sequence Name	Offset	Strandedness
RGYTACCTTGTTACGACTT	BacU_EX_11	531	+
GTGCCAGCMGCCGCGGTAA	BacU_EX_E786F	905	-
GAGTTTGATCMTGGCTCAG	Bac-U1_13	217	+
CCTACGGGNGGCWGCAG	BacU_UX_U1053F	640	-
ACTCCTACGGGAGGCAGCAGT	805r	903	+
ATCGGYTACCTTGTTACGACTTC	Bact_U2_15	1368	-

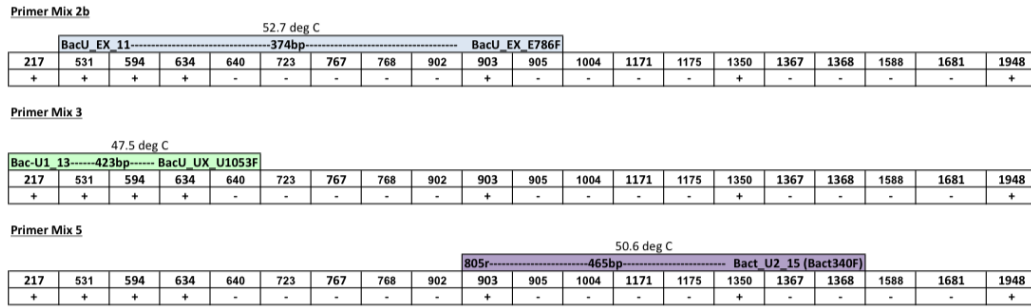


**Figure 4. 16S rRNA Primer Alignment**

SILVA rRNA gene database for bacterial domain coverage (38). Resulting sequences were then filtered using fragment lengths of 350 - 500 bases for sequencing on the Life Technologies Ion Torrent Personal Genome Machine (PGM) using the 316v2 chip. The initial BLAST search results identified alignments, offsets, and strandedness for the list of primers (Tab. 2).

Initially, six primer sets were selected from the list and evaluated using *E. coli* template. Three primer pairs with overlapping offsets were selected based upon the quantity of PCR product and length.

### 3.9 PCR

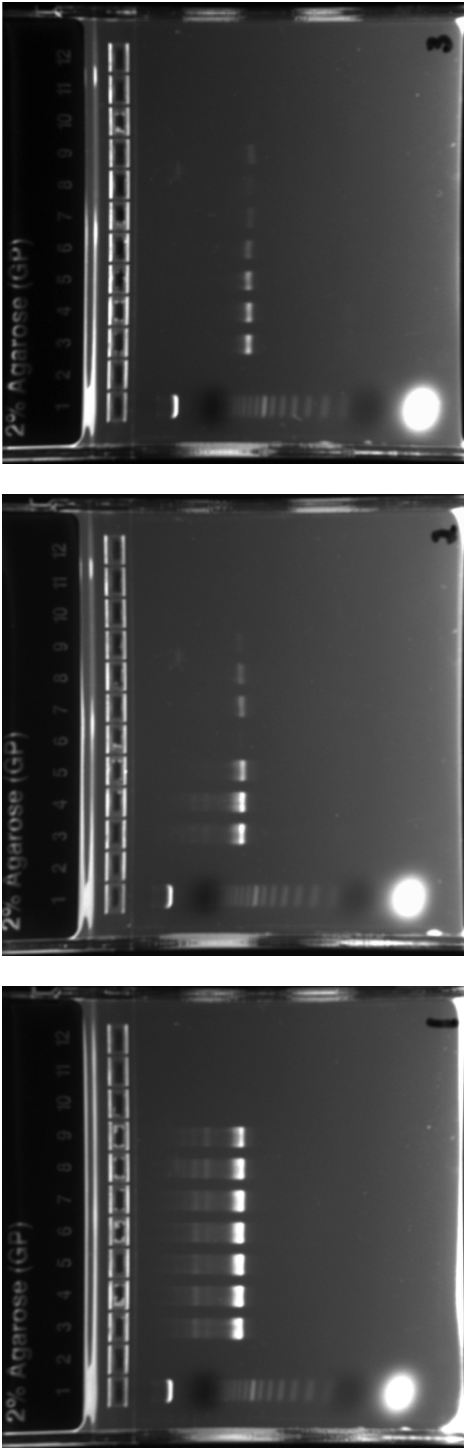
Non-barcoded, lyophilized primers (200 nmol, HPLC purified) were obtained from the list of primer pairs identified in the BLAST alignment (37) and 16S rRNA ribo-

**Table 3. Gradient PCR Profile**

Step	T (°C)	Time	Cycles
1	50	30min	
2	94	15min	
3	94	30sec	
4 (see Fig. 5)	47 - 65	30sec	
5	72	1min	
	Repeat 3 - 5		32x
6	72	15min	
7	4	$\infty$	

somal gene survey. The primers were hydrated using a TE Buffer (10 mM Tris•Cl/1 mM EDTA) to a stock solution of 100  $\mu$ M concentration. Working solutions of 20  $\mu$ M were prepared from the stock solution. The primer solutions were then placed in  $-20^{\circ}\text{C}$  storage until use.

Template DNA was obtained from laboratory stock or the reactor samples, thawed, and diluted to 10 pg/ $\mu$ L concentration. PCR reaction mixtures for each of the primer pairs were prepared using the Qiagen OneStep RT-PCR kit. The total quantity of reaction mixture was calculated for an eight reactions. 120  $\mu$ L DNA-grade water, 50  $\mu$ L 5X buffer, 10  $\mu$ L 10 mM dNTP mix, 5  $\mu$ L primer A, and 5  $\mu$ L primer B were added to the master mix tube. Once all master mixes were prepared, 10  $\mu$ L of enzyme was added to each tube and each tube was kept on ice. The master mixes were then aliquoted into eight tube strips for PCR. Five  $\mu$ L of template was added to each aliquot for a total of 25  $\mu$ L for each 0.2 mL tube reaction.



(a) EX11 E786F

(b) U113 U1053F

(c) 805R U215

T (°C)	47.0	47.5	48.7	50.6	52.7	54.9	57.1	59.3	61.4	63.3	64.5	65.0
EX11-E786F	X	X	X	X	X	X	X	X				
U113-U1053F		X	X	X	X	X	X	X	X			
805R-U215					X	X	X	X	X	X	X	X

(d) PCR Gradients

Figure 5. PCR Gradient Analysis

A temperature gradient was used to identify optimum melting temperatures ( $T_m$ ) for the initial primers without adapters or barcodes (Tab. 3). Eight-strip PCR tubes with prepared template DNA and reagent were placed in the thermocycler. The placement in the gradient PCR wells was based on GC% content and estimation from previous attempts (Fig. 5).

For the fusion primers with adapters and barcodes, the PCR temperature profile was determined using Integrated DNA Technologies' OligoAnalyzer<sup>®</sup> (39). For each search, the concentration parameters for salts and dNTPs were updated using the Qiagen OneStep RT-PCR kit manual as a reference. The primer concentration was input as 0.25 $\mu$ M. The primer pair sequences only (without adapters and barcodes) were input into the query box and the resulting  $T_m$  were reduced by 7°C. Then the primer pair sequences with adapters and barcodes were input and resulting  $T_m$  were reduced by 10°C. These values were used in PCR for the fusion primers and reactor sequencing (Tab. 5). The PCR profile is shown in Table 4.

### 3.10 Gel Electrophoresis

The products from PCR were evaluated using gel electrophoresis. The tests were run on E-Gel<sup>®</sup> single or double comb, 2% agarose, ethidium bromide stained, precast gels on an E-Gel<sup>®</sup> PowerBase<sup>™</sup> using a TrackIt<sup>™</sup> 50 bp DNA Ladder. The DNA ladder was diluted 1:4 in a 1.5 mL tube, vortexed and placed in a microcentrifuge tube rack. The required number of precast gels were obtained from laboratory stock and indexed on the bottom right corner using a marker. The PCR strips containing template DNA were removed from -80°C storage and placed on ice. For the single comb tests, lanes 2, 11, and 12 were filled with 20  $\mu$ L of DNA quality water and lanes 3 - 10 were filled with 10  $\mu$ L of DNA quality water. Lanes 3 - 10 were filled with 10  $\mu$ L of DNA template. Lane 1 was filled with 20  $\mu$ L of the diluted ladder.

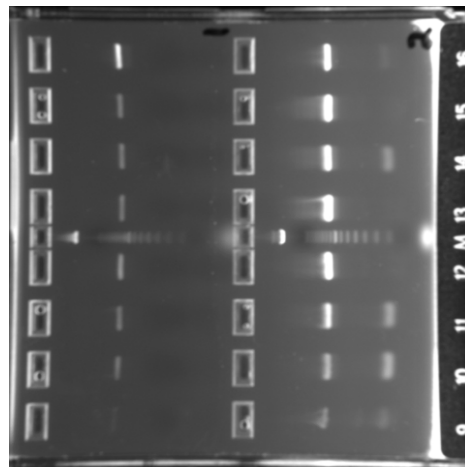
**Table 4. Sequencing Amplification Profile**

Step	T (°C)	Time	Cycles
1	50	30min	
2	94	15min	
3	94	30sec	
4	T <sub>m</sub> <sup>1</sup>	30sec	
5	72	1min	
	Repeat 3 - 5		15x
6	94	30sec	
7	T <sub>m</sub> <sup>2</sup>	30sec	
8	72	1min	
	Repeat 6 - 8		25x
9	72	15min	
10	4	∞	

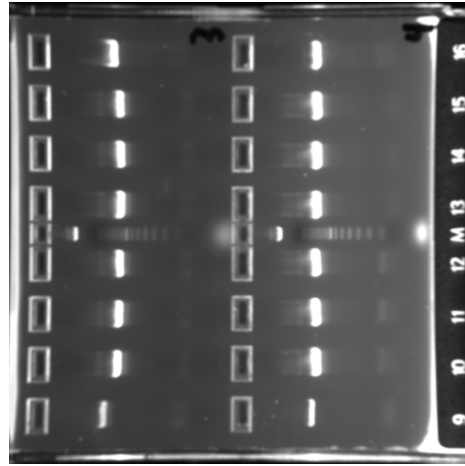
**Table 5. Sequencing Temperature Determination**

Primer	T <sub>m</sub> <sup>1</sup> (°C) Primer	T <sub>m</sub> <sup>2</sup> (°C) Primer Adapter Barcode	Bases (max)	GC content (%)
BacU_EX_11	75	81.6	64	54.7
BacU_EX_E786F	57.8	78.3	48	54.2
Selected T <sub>m</sub> (°C)	50.8 (15x)	68.3 (25x)		
Bac-U1_13	67.5	79.4	57	51.8
BacU_UX_U1053F	68.1	81.6	46	63
Selected T <sub>m</sub> (°C)	60.5 (15x)	69.4 (25x)		
805r	63.1	79.4	56	53.6
Bact_U2_15	71.8	81.7	49	61.2
Selected T <sub>m</sub> (°C)	56.1 (15x)	69.4 (25x)		

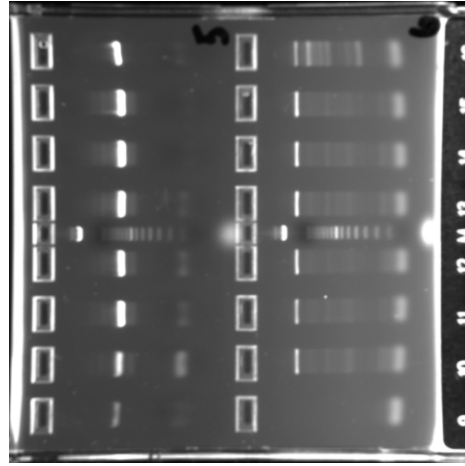
For the double comb tests, lanes 2 - 4, 5 - 7, 10 - 12, and 13 - 15 were filled with 10  $\mu$ L of DNA template (Fig. 6). Lanes 8 and 16 were filled with *E. coli* template as the positive control. Lanes 1 and 9 were the negative control. Diluted ladder was added to the middle (M) lane. The gel was then placed on the E-Gel<sup>®</sup> PowerBase<sup>™</sup> and a 30 min timer was started. After 30 min, the precast gel with the sample was removed and placed under UV transillumination using a Kodak Gel Logic 200 Imaging System. The DNA template lanes were evaluated for clarity at the target lengths and optimal temperature ranges noted.



(a) Primer Set 2: 374bp



(b) Primer Set 3: 423bp



(c) Primer Set 5: 465bp

**Figure 6. Gel Electrophoresis**



### 3.11 Adapter and Barcode Ligation

Once successful PCR products were shown using gel electrophoresis, adapters and barcodes were attached to the DNA. Ligation was only used when fusion primers (with adapters and barcodes already attached) were not used. The Ion 16S<sup>TM</sup> Metagenomics kit workflow was used as guidance for workflow for the remainder of the library construction (40). The Ion Plus gDNA Fragment Library Preparation kit, barcode adapters and protocol were used during the initial phase of sequencing parameter identification (41). The reaction was setup for a barcoded library using additional polymerase. 41  $\mu$ L of nuclease-free water was added to a 0.2 mL PCR tube. 10  $\mu$ L of 10X ligase buffer was added to the reaction mixture. 2  $\mu$ L each of Ion P1 adapter, Ion Xpress<sup>TM</sup> Barcode X, and dNTP mix were then added. The gDNA input was 100 ng at 25  $\mu$ L. Finally, 2  $\mu$ L of DNA ligase and 16  $\mu$ L of nick repair polymerase were added bringing the total reaction volume to 100  $\mu$ L. The reaction tube was then placed in a thermocycler programmed with a preheated lid at 95°C for 3 min, 25°C for 15 min, 72°C for 5 min with a final hold at 4°C. The reaction was removed from the thermocycler once the temperature reached 4°C and purified using the Agencourt<sup>®</sup> AMPure<sup>®</sup> XP Reagent kit.

### 3.12 Purification

Purification using the Agencourt<sup>®</sup> AMPure<sup>®</sup> XP Reagent kit consisted of attaching the gDNA to beads, removal of the supernatant, a series of ethanol washes, and elution using a TE buffer. Prior to beginning the purification step, a fresh mixture of 70% ethanol and 30% nuclease-free water was prepared. The sample volume was measured using a pipette. A 1.8X sample volume (180  $\mu$ L) of AMPure<sup>®</sup> beads was obtained from 4°C storage and allowed to come to room temperature for 30 min (41). The sample and beads were combined in a 1.5 mL Eppendorf LoBind<sup>®</sup> tube and mixed

using a 200  $\mu\text{L}$  pipette 5 times. The mixture was incubated at room temperature for 5 min. The mixture was pulse spun and placed in a magnetic tube rack until the solution cleared. The supernatant was withdrawn from the bead pellet and 500  $\mu\text{L}$  of the ethanol mixture was added. The tube was rotated slowly in the rack over a period of 30 sec and the ethanol wash was removed using a pipette. The ethanol wash was repeated a second time. After removal of the wash solution using a pipette, the tube was removed from the rack, pulse spun, and placed back in the rack. The remaining ethanol wash was removed using a 20  $\mu\text{L}$  pipette. The tube was left open to the air for a period of 4.5 min to allow the remaining wash to evaporate. The tube was removed from the rack and 40  $\mu\text{L}$  of TE buffer was added directly to the pellet. The buffer and beads were mixed using a pipette 10 times. The tube was pulse spun and placed in the magnetic rack until the solution cleared. The supernatant contained the gDNA was removed in two 20  $\mu\text{L}$  volumes into 2 LoBind<sup>®</sup> tubes. Both tubes were placed in  $-80^{\circ}\text{C}$  storage.

### 3.13 Size Selection

Size selection of the purified and adapter ligated and barcoded gDNA was conducted using the Pippin Prep<sup>®</sup> instrument and 2% agarose and ethidium bromide gel cassettes with external marker B and manufacturer's protocol (42). Prior to operation, the reagents for the kit were removed from  $4^{\circ}\text{C}$  storage and allowed to come to room temperature for 30 min. Loading buffer was added to the sample to bring the sample volume to 40  $\mu\text{L}$ . The Pippin Prep<sup>®</sup> instrument was calibrated using the calibration optical fixture. The cassette was removed from its packaging and inspected for proper condition. It was tilted and all air bubbles were dislodged to the right side of the cassette. The cassette was placed in the instrument tray and both tape tabs were removed. Approximately 40 - 50  $\mu\text{L}$  was removed from each elution well and

replaced with fresh electrophoresis buffer. The tape tab from the kit was then placed over the elution wells. Fresh electrophoresis buffer was added to each sample port until full. A current test was performed and all wells of the cassette passed. A program with cut sizes matching the base pair size targets  $\pm 35$  bp was added and loaded for the cassette. The reference lane was designated as lane 1 and applied to all sample lanes. The instrument was opened and 40  $\mu\text{L}$  removed from each of the sample lanes and the reference lane. 40  $\mu\text{L}$  of sample was added to each sample lane and 40  $\mu\text{L}$  of reference ladder was added to the reference lane. The instrument lid was closed and the program was started and ran for approximately 1.5 hours. Once the program completed, the sample fractions (about 40 $\mu\text{L}$ ) were removed from the elution wells. The fractions were purified using the Agencourt<sup>®</sup> AMPure<sup>®</sup> XP Reagent kit. The purification protocol was identical to the previous protocol (41). After purification, the samples were placed in  $-80^{\circ}\text{C}$  storage.

### 3.14 Quality Control and Normalization

Quality control of the samples was conducted using the Agilent Technologies Bioanalyzer 2100 and protocol (43). Samples were removed from  $-80^{\circ}\text{C}$  storage and, along with the high sensitivity DNA analysis reagents, were allowed to come to room temperature for 30 min prior to beginning the analysis. The electrode assembly was removed from the Bioanalyzer and sonicated for 10 min and dried using compressed air. The electrode assembly was returned to the Bioanalyzer system. A chip was loaded into the chip priming station and the plunger on the priming syringe was set to 1 mL. 9  $\mu\text{L}$  of gel-dye mix from the high sensitivity DNA analysis reagent kit was added to the gel priming well. The priming station was closed and the syringe depressed until locked into place by the priming station clip. Exactly 1 min later, the clip was released and 5 sec later the syringe plunger was slowly withdrawn to the 1

**Table 6. Region Table**

Sample Name	Average Size [bp]	Conc. [pg/l]	Molarity [pmol/l]	% of Total
EX_11-E786F	466	30,269.88	98,548.50	40
U1_13-U1053F	395	22,200.29	85,826.00	71
805R-U2_15	512	1,226.50	3,636.30	53

mL position. The chip priming station was opened. 9  $\mu$ L of gel-dye mix was added to the remaining gel wells. 6  $\mu$ L of marker was added to all wells without samples and 5  $\mu$ L added to all sample wells. 1  $\mu$ L of ladder reagent was added to the ladder well. Finally, 1  $\mu$ L of each sample was added to each sample well. The chip was placed in a chip-specific vortex at 2,000 rpm for 1 min. The chip was immediately loaded into the Bioanalyzer 2100 system. The Bioanalyzer program was programmed to use the high sensitivity DNA analysis protocol, the program was initiated and ran for 45 min.

Using the analysis from the quality control using the Bioanalyzer 2100, the gDNA input from each of the the primer pair PCR products was normalized. Each of the products, after size selection and purification, were evaluated according to the molarity measurement from the region table from the Bioanalyzer instrument (Tab. 6). The region analysis was conducted by assigning ranges based upon the peak readings at the highest values displayed (Fig. 7). The low value before the rise in the highest peak, The high value was after highest peak declined to a value close to the null value. The region quantitation was input into a spreadsheet. A dilution value was assigned to normalize each of the values. The molarities were then equalized to a volume  $\pm 1$   $\mu$ L at 10  $\mu$ L of common volume. Each primer was normalized to equivalency at 45 - 52 pM concentration for library input into emulsion PCR.

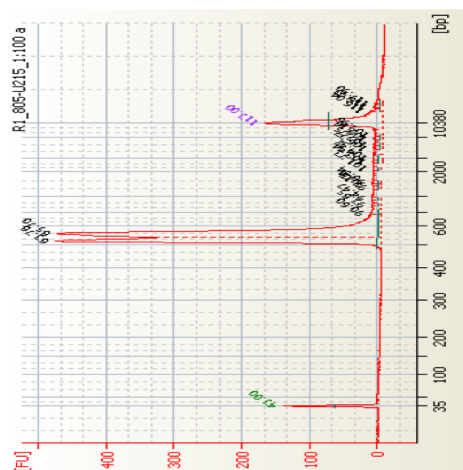
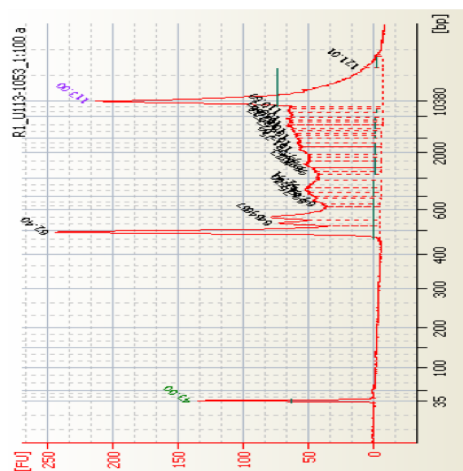
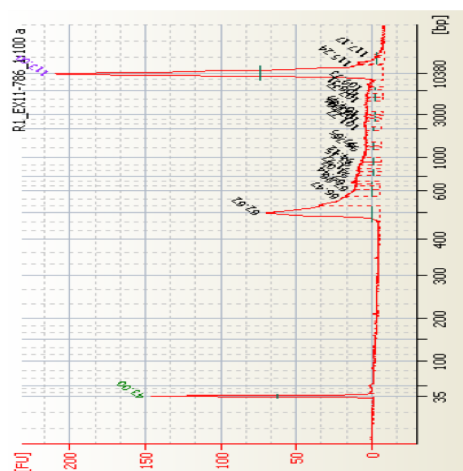


### Figure 7. Nucleic Acid Quantitation

### 3.15 Emulsion PCR

The Ion OneTouch<sup>™</sup> instrument was used to amplify the solution for sequencing using the manufacturer's protocol (44). The lid of the instrument was opened and a recovery tube installed into the slots. A recovery router was installed. The instrument lid was closed. A new amplification plate, tubing, and disposable injector were installed. Recovery solution and oil were added to bring the volumes to the designated levels. All reagents were allowed to come to room temperature prior to use. The reagent mix, Reagent B, Enzyme Mix, and Reagent X were prepared and added to the solution according to the protocol. 25  $\mu$ L of normalized solution was added to the mixture for a total volume of 900  $\mu$ L. The mixture was combined by mixing using a pipette. 100  $\mu$ L of Ion Sphere Particles (ISPs) was added to the mixture. The mixture was combined by mixing using a pipette. The complete solution was then added to a Ion PGM<sup>™</sup> OneTouch<sup>™</sup> Plus Reaction Filter Assembly via the sample port. 1500  $\mu$ L of reaction oil was then added via the sample port. The filter assembly was then inverted and installed on the OneTouch<sup>™</sup> instrument. The OneTouch<sup>™</sup> instrument was then initiated using the Ion PGM<sup>™</sup> Template OT2 400 Kit protocol assist and ran for 7.5 hrs. A final spin was conducted at the completion of the run and the ISPs processed. Processing included removal of the recovery tubes and solution to 100  $\mu$ L. The ISPs from both recovery tubes were suspended in 500  $\mu$ L of Ion OneTouch<sup>™</sup> Wash Solution, dispersed, and stored at 4°C.

### 3.16 ISP Quality Control and Enrichment

The ISPs were incubated at 50°C for 2 min. The ISPs were then centrifuged at 15,500 x g for 2.5 min and all but 100  $\mu$ L of wash solution removed. The quality of the the ISPs was evaluated using the Qubit<sup>®</sup>. The Ion Sphere<sup>™</sup> Quality Control kit Ion Probes, Annealing Buffer, and Quality Control Wash Buffer were thawed. A 2

$\mu\text{L}$  aliquot of the unenriched ISPs was transferred to a 0.2 mL Eppendorf PCR tube and brought to room temperature with 98  $\mu\text{L}$  of Ion OneTouch<sup>™</sup> Wash Solution. 2  $\mu\text{L}$  was transferred to a 0.2 mL Eppendorf PCR tube. 19  $\mu\text{L}$  of annealing buffer, 1  $\mu\text{L}$  of Ion Probes were added to the tube and mixed with a pipette. The tube was loaded into a thermocycler with a heated lid set a 95°C, 95°C for 2 min, and 37°C for 2 min. The unbound probes were washed three times with 200  $\mu\text{L}$  of Quality Control Buffer by adding 200  $\mu\text{L}$ , mixing with a pipette, centrifuging at 15,500 for 1.5 min and removing the supernatant. 10  $\mu\text{L}$  was left in the tube using a comparison tube as a reference. After the final wash, the volume was brought to 200  $\mu\text{L}$  and mixed using a pipette. The entire volume was transferred to a Qubit<sup>®</sup> assay tube. A negative control was produced using a similar volume without sample. Alexa Fluor<sup>®</sup> standards 488 and 647 were measured on the Qubit<sup>®</sup> fluorometer. The negative control and sample containing the ISPs were then measured in both 488 and 647 settings. The values for the standards, control, and sample were then input into the calibration factor spreadsheet from the manufacturer's website to calculate the percent templated ISPs. A value between 10 - 30% was the optimal templated ISPs goal. The manufacturer's recommended molarity of 26 pM appeared to correlate with the lower end of this optimal range. A molarity of 26 - 52 pM was utilized during this study.

Following a successful quality control evaluation, the ISPs were enriched on the Ion OneTouch<sup>™</sup> Enrichment System (ES) using the manufacturer's protocol (44). A 1 mL volume of 1M NaOH was prepared by diluting 10M NaOH using water from the sequencing kit. A second 1 mL volume of 100mM NaOH was prepared in the same way and set aside for use later in sequencing. A melt-off solution was prepared by combining 280  $\mu\text{L}$  of Tween<sup>®</sup> solution with 40  $\mu\text{L}$  of 1M NaOH. Dynabeads<sup>®</sup> MyOne<sup>™</sup> Streptavidin C1 Beads were removed from storage and resuspended using a vortex. 13  $\mu\text{L}$  were removed and added to a 1.5 mL Eppendorf LoBind<sup>®</sup> tube. The tube

was then placed on a magnetic rack for 2 min and the supernatant removed. 130  $\mu\text{L}$  of MyOne<sup>TM</sup> Bead Wash Solution was added, vortexed and briefly centrifuged. The 8-well strip from the Ion OneTouch<sup>TM</sup> kit was prepared with the square-shaped tab on the left. Wells 3, 4, and 5 were filled with 300  $\mu\text{L}$  of Ion OneTouch<sup>TM</sup> wash solution. Well 7 was filled with 320  $\mu\text{L}$  of the freshly prepared melt-off solution. Well 2 was filled with 130  $\mu\text{L}$  of MyOne<sup>TM</sup> Beads Wash Solution with MyOne<sup>TM</sup> Beads. Well 1 was filled with the entire volume of sample template-positive ISPs ( $\sim 100$   $\mu\text{L}$ ) from the emulsion PCR step. The strip was loaded into the right side of the slot in the tray of the enrichment system with the square tab to the left. A new tip was installed in the tip arm and a 0.2 mL with 10  $\mu\text{L}$  of neutralization solution placed in the hole of the tip loader. The enrichment cycle was initiated and ran for approximately 35 min. Immediately following enrichment, the solution was mixed in the PCR tube with the neutralization solution by pipetting up and down 10 times. The PCR tube with the enriched beads was then placed on ice.

### 3.17 Sequencing

The sequencing solutions for Wash 2 and Wash 3 and annealing buffer were removed from storage and brought to room temperature in a closed drawer. The dNTPs, sequencing primer, and control Ion Sphere<sup>TM</sup> Particles (ISPs) were placed in an ice bucket to thaw. A cleaning cycle was performed on the Ion PGM<sup>TM</sup> sequencer using either the chlorite protocol or the the water rinse. The chlorite protocol was used once per week and the rinse used for daily uses. A previously designated, used initialization Ion 316<sup>TM</sup> v2 chip was placed in the sequencer for the initialization step. The three wash bottles from the 400 kit were washed 3 times using 18.2 $\Omega$  water and inverted to dry. The wash bottle sipper tubes were then removed and the 400 kit selected on the sequencer screen. The sequencer verified gas pressure after screen confirmation and



a glove change was completed. New sipper tubes with the gray tops were attached with the long W2 tube resting on a sterile gauze patch. 350  $\mu\text{L}$  of 100 mM NaOH was added to the Wash 1 bottle, which was then capped. 50 mL of Wash 3 solution from the kit was added to the Wash 3 bottle and the bottle capped. 2 L of 18.2M water, the entire bottle of W2 solution from the kit, and 70  $\mu\text{L}$  of 100 mM NaOH was added to the Wash 2 bottle, which was then capped and mixed by inverting 5 times. The Wash 2 bottle was then attached, followed by the Wash 1 and Wash 3 bottles and the caps secured. The initialization process continued. The pH was monitored until initialization was complete to allow for manual adjustment using titration.

After initialization completed successfully, the next step was preparing the dNTP bottles. The dNTP reagent bottles were designated using their respective stickers. 20  $\mu\text{L}$  of each dNTP was added to its designated bottle by placing the pipette tip approximately one third of the way down against the inside wall and depressing the pipette plunger. The bottles were then capped and placed in racks. The old sipper tubes were removed from the dNTP ports and a glove change was conducted. New sipper tubes with blue tops and the appropriate dNTP bottles were then firmly secured to the ports. The machine then conducted a leak test and the dNTP bottles filled.

After the dNTP bottles were prepared, the control Ion Sphere<sup>TM</sup> particles were added and the sequencing primer was annealed. The control particles were vortexed and centrifuged and 5  $\mu\text{L}$  of control particles added to the PCR tube from the enrichment. The solution was then mixed with a pipette and centrifuged for 2 min at 15,500 x g. The supernatant was removed, leaving 15  $\mu\text{L}$  in the tube by using another tube for comparison. 12  $\mu\text{L}$  of sequencing primer was added. The total volume was verified using a pipette and additional annealing buffer added as required. The solution was then mixed using a pipette. The PCR tube was then loaded into a thermocycler at

95°C for 2 min and 37°C for 2 min using the heated lid option.

While the PCR program was running, the sequencing run was programmed using the administrative interface in a web browser. The appropriate chip type (316v2), generic sequence, and no reference library were selected. The run and sample identifications were input, along with designating the appropriate kits used. Finally, the program was saved and verified under the “Plan run” selection.

The last preparation step prior to initiating the sequencing run was to conduct a chip check and load the chip. At this point, gloves were removed to prevent static discharge that would damage the chip. The initialization chip was removed from the sequencer after touching the grounding plate. A new 316v2 chip was removed from its packaging and placed in the sequencer. The barcode was read by the scanner and chip check initiated on the touchscreen. After a successful chip check, sequencing polymerase was removed from storage. The sample with ISPs and primer was removed from the thermocycler. 3  $\mu$ L of polymerase was added to the sample by rotating the pipette pusher to avoid any bubbles. The sample with polymerase was then mixed using the pipette and allowed to incubate at room temperature for 5 min. The sequencing chip was then removed from the sequencer and all liquid removed from the chip. The loading procedure used was the alternate method using simplified instructions and the weighted chip bucket. This involved centrifuging the chip upside down in the weighted bucket for 5 sec. The 30  $\mu$ L sample was then loaded into the chip by rotating the pipette pusher at a rate of 1  $\mu$ L per second to prevent any bubbles entering the chip. The chip was then placed in the weighted bucket and centrifuged with the chip tab in for 1 min and then centrifuged again with the chip tab out for 1 min. The chip tab was then tapped on the bench top 3 times and liquid was removed from the chip loading port by rotating a pipette pusher until no more liquid entered the pipette tip.

The sequencing run was then initiated by selecting the run, loading the chip, and initiating the run. The planned run that had been previously programmed was selected, the settings reviewed, and confirmed. After grounding, the chip was loaded, clamped and the cover closed. The sequencer calibrated the chip and the sequencing run was initiated. The sequencing run time was approximately 5 hours. The process of constructing a library, preparing the templated ISPs and sequencing was repeated for each reactor two times.

### **3.18 Bioinformatics**

After sequencing, a Binary Alignment/Map (BAM) file was generated with raw sequencing data from the run. The SAMtools 0.1.18 utilities suite was used to interact with and conduct immediate post-run processing of the BAM file (45). Sequence adapter trimming was accomplished using Cutadapt 1.2.1 (46). Quality control and assembly of the sequence reads was conducted using Mira 3.9.1.7 (47). The resulting three output files were generated with FASTA, FASTQ, and QUAL extensions.

A standalone version of NCBI's BLAST 2.2.30+ was downloaded along with the 16S Microbial database (37). The add-on taxonomy database was also loaded to include additional information for reference. Using the command line interface, the FASTA files for each barcode set of contiguous (contig) sequences were parsed using a nucleotide query (blastn) and NCBI's 16S microbial database. The BLAST query used default standalone values and was output in XML format.

The BLAST output file was then imported into MEGAN (48). A Least Common Ancestor (LCA) parameter filter was applied. The minimum bit score for results was 50.0. The maximum expected value (e-value) was 0.01. All returned values below 10.0% of the maximum percentage hit were discarded. No minimum percentage or number of reads was set. Finally, the 16S Percent Identity Filter was enabled enforcing

rank-based match percentage requirements of Species 99%, Genus 97%, Order 90%, Class 85%, and Phylum 80%. Under the Taxonomy tab, the Parse Taxon Names feature was enabled. The BLAST output file was then imported. Once all BLAST outputs were imported for a reactor, the resulting trees were compared to assess the differences between reactor taxa compositions and supporting contig counts.

## IV. Results and Analysis

### 4.1 Sequencing

**Table 7. Sequencing Run Data**

	Reactor 1	Reactor 2	Reactor 3
ISP Loading	59%	72%	56%
Total Bases Read	116,000,000	560,000,000	404,000,000
ISP Not Templated	(10%)	0%	(8%)
ISP Polyclonal	(36%)	(25%)	(36%)
ISP Low Quality	(66%)	(8%)	(20%)
Useable Reads	728,779	3,128,271	1,680,002
Useable Reads (%)	22%	69%	52%
Read Mean Length/Median/Mode (bp)	160 / 88 / 29	179 / 99 / 41	241 / 242 / 450
Total Contigs	497	484	233
Mean Contig Length (bp)	416	395	385
Mean Reads per Contig	338	326	392

Six sequencing runs were conducted in total. Three runs were selected after filtering by post-sequencing quality checks (Tab. 7). The initial total number of reads was filtered to ensure the optimal quality for downstream analysis. The most efficient product was obtained from Reactor 2, producing 69% useable reads from 72% ISP loading and 560 million reads. Reactor 1 produced the most contiguous sequences at 497 total contigs after sequencer- and software-based quality checks. Reactor 3 produced the fewest contigs at 233, but had the most overall mean reads per contig at 392, and the highest read length parameters. A graphical summary is shown in Figures 8(a) - 10(a). The highest ISP density is shown in red, with decreasing values in yellow, green and blue, respectively. The proportion of the run length associated with the target  $\sim 490$ bp region is identified by a peak on the right of the histogram (Fig. 8(c) - 10(c)).

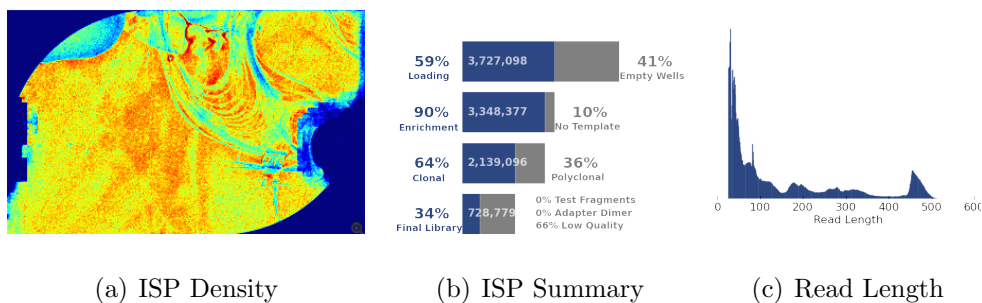


**Figure 8. Reactor 1 Sequencing Data**

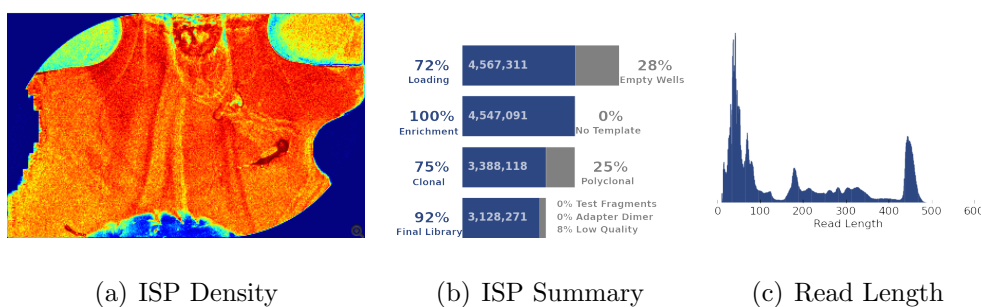


**Figure 9. Reactor 2 Sequencing Data**

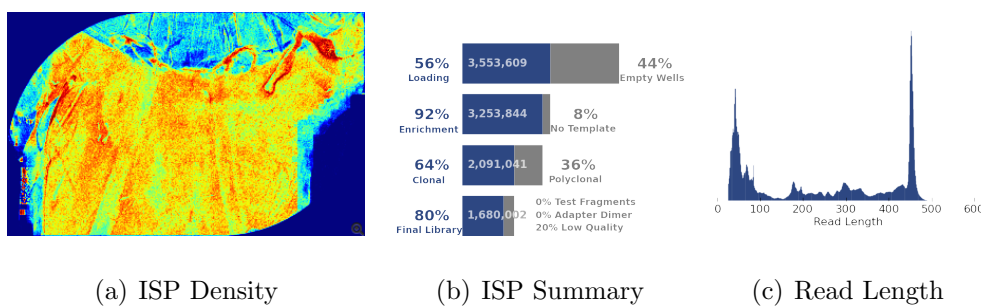


**Figure 10. Reactor 3 Sequencing Data**

## 4.2 Nitrification

Reactor nitrification and suspended solids data are summarized in Figures 11 - 13. Average values for each were compared for the early, acclimation, late, and malathion addition periods between Days 1 - 90, 91 - 170, 171 - 250, and 251 - 283, respectively. The average sludge retention time (SRT) for across all periods for all three reactors was 19 ( $\pm 6$ ) days. The average pH values for Reactors 1, 2, and 3 were 7.16, 6.99, and 7.27, respectively.

In all three reactors, the ratio of effluent TSS to mixed liquor TSS was high during the early period. In Reactors 1 and 3, this coincided with high values of TSS in the effluent at  $124 \frac{mg}{L}$  and  $70 \frac{mg}{L}$ , respectively, and in Reactor 2 with low values for TSS in the mixed liquor at  $1144 \frac{mg}{L}$ .  $NO_2^-$  concentrations were high for all reactors, but more so in Reactors 2 and 3, with 82% of nitrite remaining in the effluent for both compared to the starting mixed liquor value at the beginning of a 12-hr cycle. This may have indicated low overall proportions of NOB, with the effects amplified by subsampling to seed Reactors 2 and 3. Finally, COD concentrations in the effluent were highest for Reactor 3 for this period at  $23.99 \frac{mg}{L}$ , suggesting a lower proportion of heterotrophs. The results show a disruption of the recently established equilibrium achieved in Reactor 1.

During the acclimation period, the total biomass in Reactor 1 dropped to 74% of the higher mixed liquor TSS value. In Reactor 2, a higher than average value of 50% of COD remaining the effluent compared to the mixed liquor was observed.  $NH_4-N$  concentrations were low in the reactor and zero in the effluent. Nitrate levels were lower in the effluent than in the mixed liquor, which may have been the result of denitrification activity. In Reactor 3, lower than average  $NH_4-N$  removal and excess  $NO_2^-$  in the mixed liquor and effluent indicated degraded nitrifying activity. These measurements show that the seeding of Reactor 2 and 3 involved unequal distribution

of nitrifying and heterotrophic groups into those reactors.

In the late period just before the addition of malathion, SRT was lower in all three reactors at 14 days.  $\text{NH}_4\text{-N}$  and  $\text{NO}_2^-$  levels in Reactor 1 reached a peak value in the starting mixed liquor value in comparison to the other periods, but the values of both were zero in the effluent. This corresponded with an average of  $29 \frac{\text{mg}}{\text{L}}$  nitrate in the effluent. In Reactor 2, all values were within one deviation of the mean across all periods. In Reactor 3, the mean effluent COD concentration dropped to its lowest value at  $15.86 \frac{\text{mg}}{\text{L}}$ , indicating an active heterotroph community. Effluent  $\text{NH}_4\text{-N}$  and  $\text{NO}_2^-$  concentrations were both zero and nitrate levels averaged  $28.76 \frac{\text{mg}}{\text{L}}$ . For all three reactors, the communities appeared to have reached an equilibrium structure.

Finally, malathion was added to the feed of Reactor 3 on Day 242 with a concentration that achieved  $3.0 \frac{\text{mg}}{\text{L}}$  in the mixed liquor. In Reactor 1, it was added to achieve  $0.1 \frac{\text{mg}}{\text{L}}$  on Day 255. Monitoring continued until Day 283. In Reactor 1,  $\text{NO}_2^-$  concentrations were present in the effluent 6 days after malathion was added, but returned to zero 5 days later. Average effluent COD levels for this time period were lower at  $12.5 \frac{\text{mg}}{\text{L}}$ . These measurements indicate some level of negative impact to the NOB, but continued metabolic activity among the heterotrophs. However, Reactor 2, which was maintained without adding malathion, showed low effluent COD concentrations and expected concentrations of  $0 \frac{\text{mg}}{\text{L}}$  for both  $\text{NH}_4\text{-N}$  and  $\text{NO}_2^-$ . In Reactor 3, the mixed liquor COD concentration was elevated at  $65 \frac{\text{mg}}{\text{L}}$ . It may be that at  $3.0 \frac{\text{mg}}{\text{L}}$  malathion, heterotrophs begin to exhibit a stress response towards the new substrate as described in Janeczko (2014) (1).



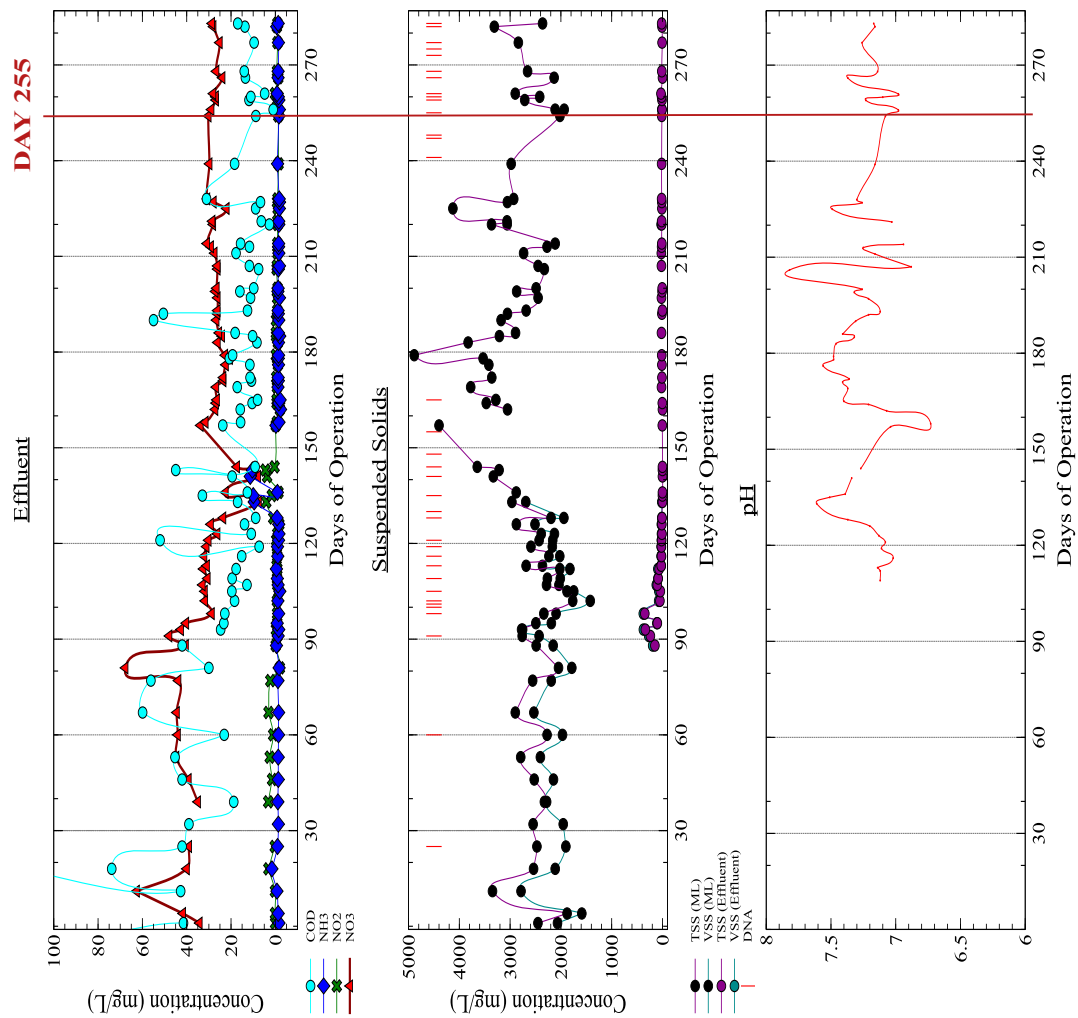


Figure 11. Reactor 1 Nitrogen, Suspended Solids, and pH

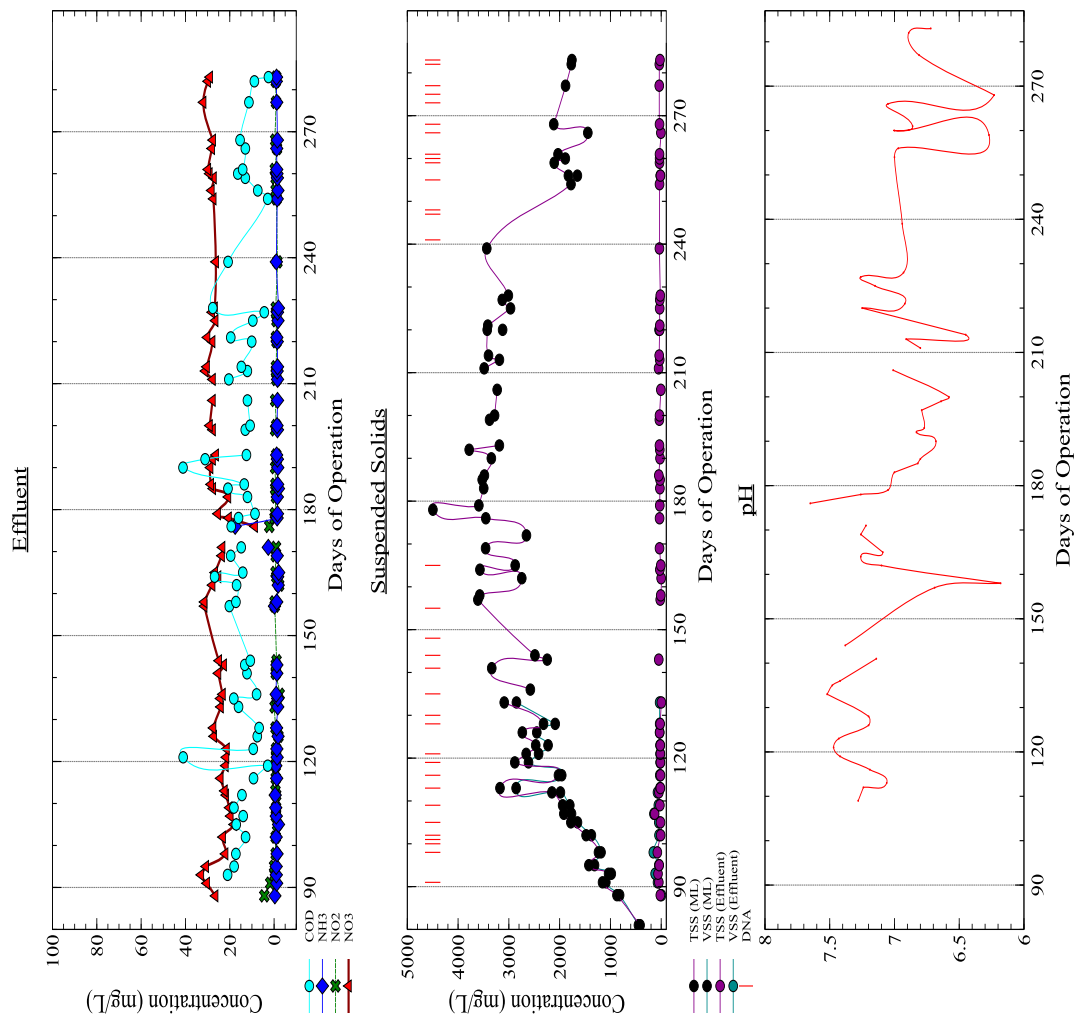


Figure 12. Reactor 2 Nitrogen, Suspended Solids, and pH

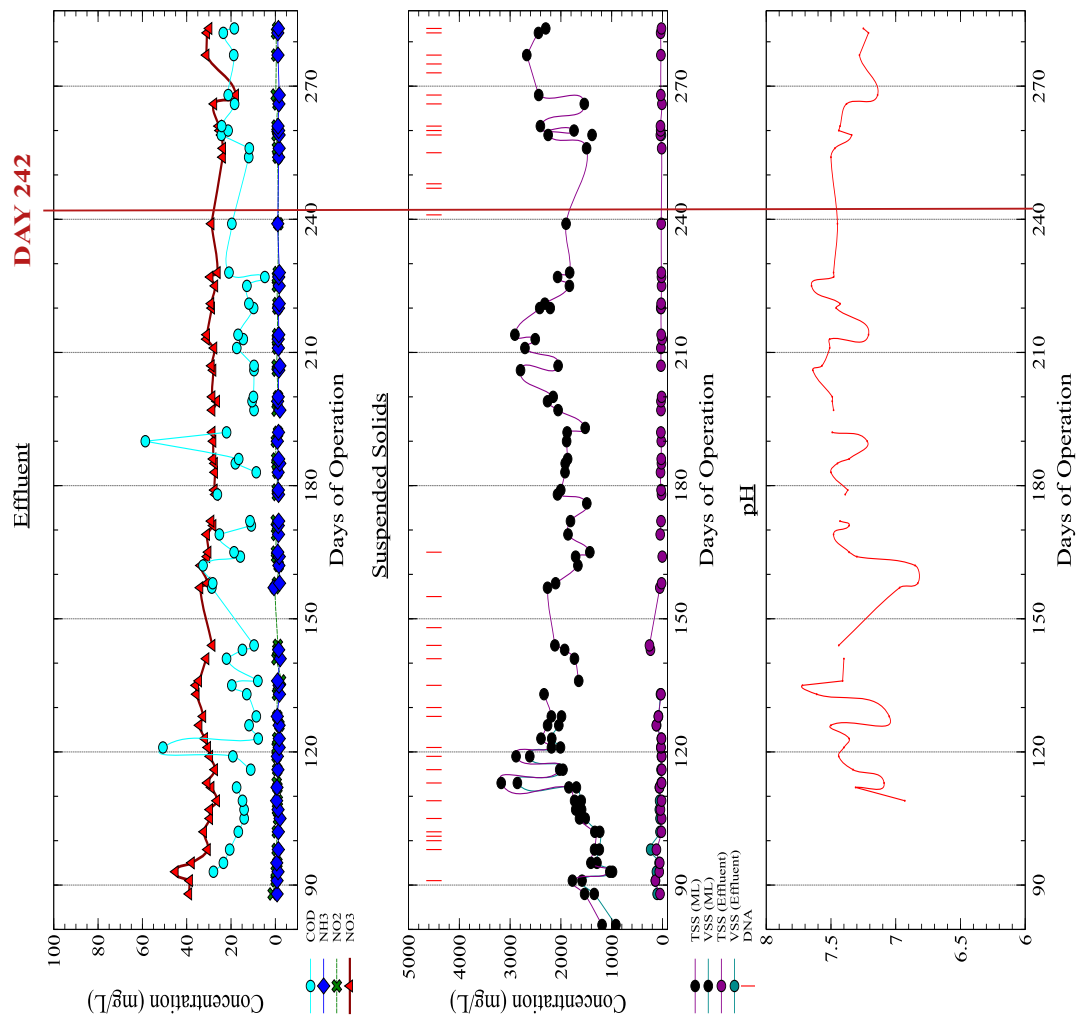


Figure 13. Reactor 3 Nitrogen, Suspended Solids, and pH

### 4.3 Bioinformatics

**Table 8. Phylogenetic Analysis Results**

	Reactor 1	Reactor 2	Reactor 3
Early/Acclim/Late or Malathion (Diversity)	15.3 / 11.6 / 8.0	9.1 / 4.5 / 3.2	5.0 / 4.0 / 3.5
Genera	37	27	22
Genera (Reads / % of total)	67 (32%)	65 (36%)	50 (40%)

The bioinformatics analysis of the three reactors described the similarities and differences between the reactors and the early, acclimation, and late or malathion addition periods. The biodiversity of each sample set was assessed using the Simpson Reciprocal Index feature in MEGAN (48). The most diverse sampling was obtained from Reactor 1 with values of 15.364, 11.636, and 8.000 for the acclimation, malathion addition, and early periods, respectively (Tab. 8). The least diverse sampling was from Reactor 3 with values of 5.000, 4.000, and 3.571, from the acclimation, malathion addition, and early periods, respectively. Reactor 2 sample values were 9.151, 4.500, and 3.267 from the acclimation, early, and late periods. These values indicate the probability of obtaining duplicate genera in any random sampling from the reactors ranged between 6.5% to 30.61%. All three reactors were associated with a temporal decline in diversity during the operational period.

For each period and reactor, a metagenomic comparison was conducted in MEGAN to associate reads with taxa. MEGAN uses similarity-based binning and reference sequences from known operational taxonomic units (OTUs) to build a tree. Sequences without annotation are placed between annotated sequences, and based on similarity, the unannotated sequence is placed nearer to the more similar annotated sequence. Assignments of reads to taxons is then conducted using LCA deduction, with non-homologs being assigned to the “no hits” category (49).

The trees shown in Figures 14 - 16 display taxonomic profiles across all three

periods. A bar chart next to each taxon displays the supporting square root normalization of reads, a recommended statistical method for phylogenetic analysis (50). The bars represent the early, acclimation, and late/malathion addition periods. Sub-taxa are not additive to higher taxa, as reads are assigned according to rank-based match percentage requirements.

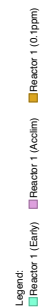


Figure 14. Reactor 1 Phylogeny

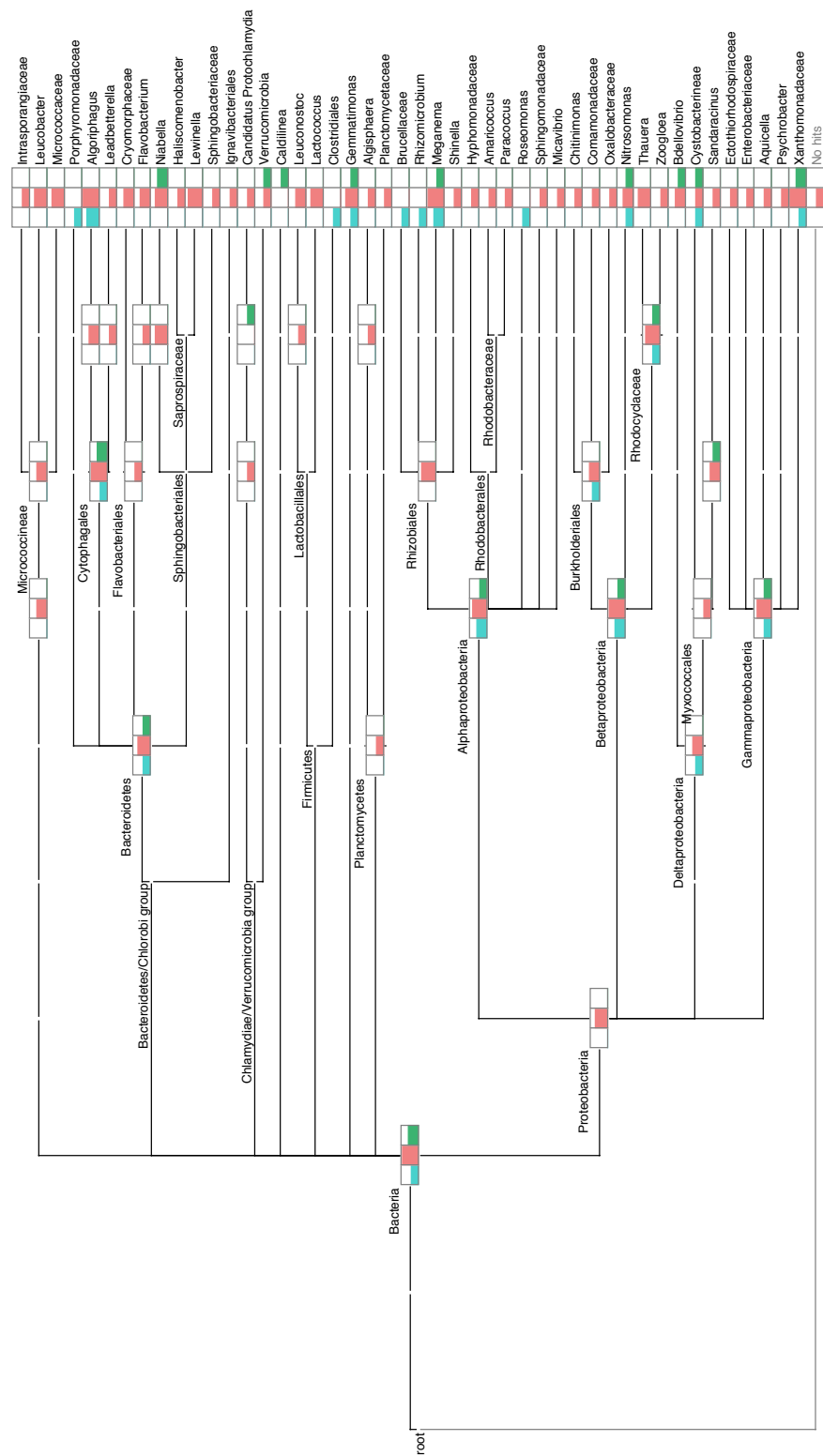


Figure 15. Reactor 2 Phylogeny

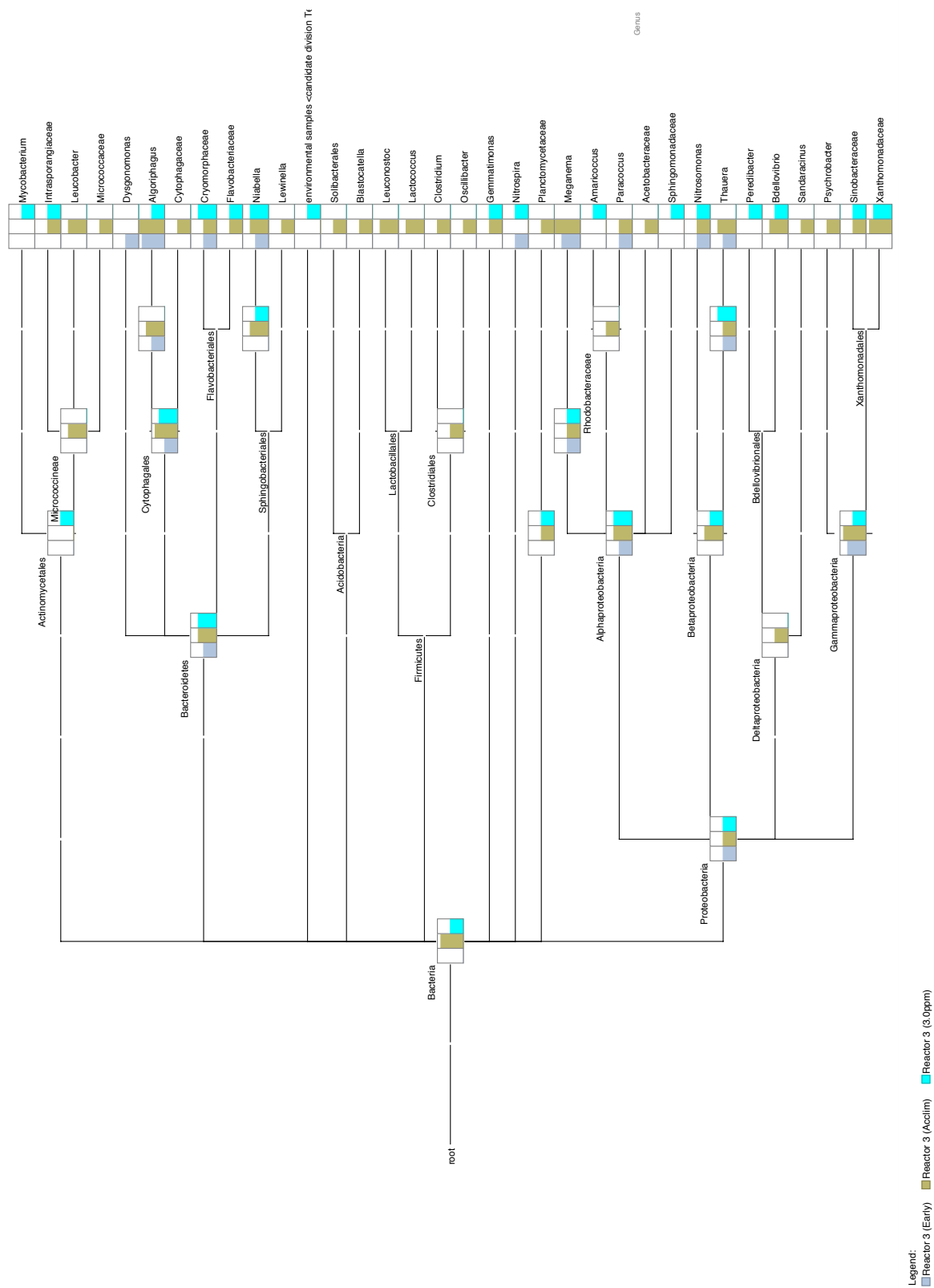


Figure 16. Reactor 3 Phylogeny



## 4.4 Analysis

A comparison of the changes in assigned reads between the early and acclimation period and the acclimation and late/malathion addition period was conducted using the ratio:

$$\frac{ReadsAssigned_1 - ReadsAssigned_2}{AverageReads_1 - AverageReads_2} \quad (6)$$

The genera most affected during the transition from the early period to the acclimation period are shown in Tables 9 and 10. The genera affected by the addition of malathion or the later period of operation (Reactor 2) are shown in Tables 11 and 12. Taxonomic groups represented in these figures are the Cytophaga-Flavobacterium-Bacteroides (CFB group), Chloroflexi (green non-sulfur bacteria or GNSB group), Actinobacteria (high GC gram positive), Firmicutes (low GC gram positive), Verrucomicrobia, Nitrospirae, and Alpha-, Beta-, and Deltaproteobacteria classes.

The first group examined is the Proteobacteria phylum, which represented the highest percentage group in all three reactors. *Meganema* is known to cause bulking in activated sludge systems and grows quickly with a high substrate affinity in high oxygen or nitrate environments (51). Along with *Nordella*, *Meganema* is a member of the Rhizobiales order, which suggests a role in nitrogen-fixation. *Bdellovibrio*, a predator, increases in high bacterial load environments and strongly affect biofilm composition (52). *Peredibacter*, another *Bdellovibrionales*, is also a predator requiring gram negative hosts in a parasitic cycle (53). It is possible that *Bdellovibrio*'s tendency to increase and decrease with *Meganema* in Tables 9 and 12 indicate a predator/prey relationship. *Thauera* is a versatile consumer of substrates, and can grow aerobically or anaerobically with nitrate, which is reduced to N<sub>2</sub>O (54). *Thauera* has also shown a capability to degrade a wide variety of aromatic compounds (55).

**Table 9. Increase after Acclimation**

Reactor 1 (Acclimation)	Reactor 2 (Acclimation)	Reactor 3 (Acclimation)
Meganema (causes bulking)	Algoriphagus (NH <sub>4</sub> degrader)	Meganema (causes bulking)
Bdellovibrio (predator)	Lewinella (biopolymer degrader)	Algoriphagus (NH <sub>4</sub> degrader)
	Meganema (causes bulking)	
	Leucobacter (pesticide degrader)	
	Thauera (aromatic degrader)	
	Lactococcus (pesticide degrader)	

**Table 10. Decrease after Acclimation**

Reactor 1 (Acclimation)	Reactor 2 (Acclimation)	Reactor 3 (Acclimation)
Crocinitomix (possible OP degrader)	Caldilinea	Peredibacter (predator)
Prostheco bacter		Amaricoccus
Lactococcus (pesticide degrader)		Mycobacterium (OPH-like gene)
Nitrosomonas (NH <sub>4</sub> to NO <sub>2</sub> )		Nitrospira (NO <sub>2</sub> to NO <sub>3</sub> )

**Table 11. Increase after Malathion**

Reactor 1 (0.1ppm)	Reactor 2 (0.0ppm)	Reactor 3 (3.0ppm)
Bryobacter (acid-tolerant)	Roseomonas	Dysgonomonas (not NO <sub>3</sub> reducing)
Pontibacter (biopolymer degrader)	Caldilinea	Nitrospira (NO <sub>2</sub> to NO <sub>3</sub> )
Cryomorpha (possible OP degrader)		
Caldilinea		
Nordella (nitrogen fixation)		
Dyadobacter (biopolymer degrader)		
Runella (biopolymer degrader)		
Amaricoccus		

**Table 12. Decrease after Malathion**

Reactor 1 (0.1ppm)	Reactor 2 (0.0ppm)	Reactor 3 (3.0ppm)
Meganema (causes bulking)	Lewinella (biopolymer degrader)	Meganema (causes bulking)
Bdellovibrio (predator)	Meganema (causes bulking)	Leucobacter (pesticide degrader)
Opiritutus (acid/anoxic)	Leucobacter (pesticide degrader)	Lactococcus (pesticide degrader)
Lewinella (biopolymer degrader)	Thauera (aromatic degrader)	Leuconostoc (pesticide degrader)
Algoriphagus (NH <sub>4</sub> degrader)	Lactococcus (pesticide degrader)	Bdellovibrio (predator)
Nitrospira (NO <sub>2</sub> to NO <sub>3</sub> )	Niabella (biopolymer degrader)	

*Americoccus* is an aerobic chemoheterotroph belonging to the family Rhodobacteraceae (56). *Roseomonas* is an oxidative bacteria associated with pathogenicity and infections (57).

*Algoriphagus*, *Dyadobacter*, *Pontibacter*, *Runella*, *Crocinitomix*, *Niabella*, *Cryomorpha*, and *Lewinella* are CFB group bacteria, the second largest representation in the reactors. CFB are chemoorganotrophic, generally aerobic, and proficient in degrading biopolymers (58). *Algoriphagus* is a member of the order Cytophagales, known for growth on peptone and organic nitrogen compounds with some groups capable of degrading inorganic nitrogen compounds such as  $\text{NH}_4$  (52). This may have been a factor in Reactor 3 where excess  $\text{NH}_4\text{-N}$  during the acclimation period contributed to the growth of *Algoriphagus*. *Dyadobacter*, *Pontibacter*, and *Runella* are also members of Cytophagales. *Lewinella* is chemoorganotroph in the Sphingobacteriales order and is strictly aerobic (59). *Crocinitomix* and *Cryomorpha* belong to the *Flavobacteriales* order (60). *Flavobacterium sp.* was the first microorganism identified that could degrade OPs (12). *Cryomorpha*, in Table 11, appears to have responded positively after the addition of malathion at  $0.1 \frac{\text{mg}}{\text{L}}$ .

Some of the groups were represented by fermentative and acid tolerant genera. *Dysgonomonas*, another CFB group bacteria, is fermentative, facultatively anaerobic, and does not reduce nitrate (61). Along with *Nitrospira*, it showed an increase in assigned reads after adding malathion. Other fermentative bacteria were negatively affected by the addition of malathion. *Leucobacter*, along with *Lactococcus* and *Leuconostoc*, are lactic acid bacteria (LAB) which are fermentative and prefer acidic environments. *Leucobacter* belongs to the phylum Actinobacteria and *Lactococcus* are members of Firmicutes. Reactor 1, which had operated for over three months, experienced a drop in *Lactococcus* reads after the transition, suggesting that a more stabilized, aerobic nitrification environment was less suitable for fermentative

bacteria. LAB have been shown to enhance the degradation of pesticides including malathion (62), but received fewer assigned reads during malathion addition in Reactor 3. This may be the result of a period of adaptation towards the substrate, or could have been affected by other processes. *Leucobacter* and *Lactococcus* were also assigned fewer reads in Reactor 2, where no malathion was added. Another genus, *Opitutus*, a Verrucomicrobia member, is also fermentative and believed to be widespread in anoxic terrestrial environments (52). The addition of a foreign substrate and the aerobic conditions in Reactor 1 may have been the cause of *Opitutus*'s decline after malathion. Finally, *Bryobacter* is slow-growing, chemoorganotroph from the phylum Acidobacteria that is strictly aerobic and also acid-tolerant (63). *Bryobacter*'s assigned reads were higher in Reactor 1 after the addition of malathion.

Another member of Verrucomicrobia is *Prostheco bacter*, an aerobic genus that has been found in ponds, lakes, and sewage (52). *Caldilinea* is a relatively recent discovery, but has been described as a GNSB-group, facultatively aerobic bacterium that grows chemoorganotrophically (64). *Caldilinea* was assigned more reads in both Reactor 1, which had  $0.1 \frac{mg}{L}$  malathion, and Reactor 2 without malathion. *Mycobacterium*, from the Actinobacteria phylum, have been associated with tuberculosis and leprosy (65). This genus also possesses the OPH-like gene, that produces the nucleotide cyclase phosphodiesterase Rv0805 (66). It is not clear whether this played a role after malathion addition, based on the number of assigned reads.

The remaining two genera, *Nitrosomonas* and *Nitrospira*, are nitrifying bacteria. *Nitrosomonas* decline in Reactor 1 after acclimation is not reflected in the nitrification data. However, the total biomass had dropped to 74% of the higher mixed liquor TSS value, possibly as a result of seeding Reactors 2 and 3. In Reactor 2, during acclimation,  $NH_4-N$  was low in both the effluent and the reactor, suggesting that AOB were active. In Reactor 3, effluent  $NH_4-N$  was present, suggesting a low population

of AOB. It is likely, therefore, that AOB were distributed primarily to Reactor 2. Effluent nitrite concentrations were lower and nitrate concentrations normal in Reactor 3 during the acclimation period, corresponding with a decrease in assigned reads to *Nitrospira*. This suggests that the slow-growing, low population of AOB was unable to sustain the initial population of NOB, causing a drop during acclimation. The decrease in *Nitrospira* reads in Reactor 1 is associated with the short-term rise in nitrite concentration six days after the addition of malathion. However, in Reactor 3 where the concentration of malathion was  $3 \frac{mg}{L}$ , no similar decline in reads was identified for *Nitrospira*. *Nitrospira* reads were higher for Reactor 3 after the addition of malathion. Janeczko (2014) suggested that partial heterotrophic decline may have enabled other unaffected groups to increase and along with those able to metabolize malathion (1). If *Meganema*, a species known for bulking, and *Bdellovibrio*, a predator, declined, as shown in Table 12, this may have been the case.

## V. Conclusions

This research has provided insight into the interactions within bacterial communities exposed to malathion, a commercial pesticide and organophosphate. Diversity was highest in the reactor seeded directly from the wastewater treatment plant with an initial Simpson's Reciprocal Index value of 15.3. Temporal decline in diversity was observed in all three reactors. Ammonia-oxidizing bacteria exposed to malathion for 30 days at  $0.1 \frac{mg}{L}$  and  $3.0 \frac{mg}{L}$  were not significantly affected. Nitrite-oxidizing *Nitrospira* was associated with increased reads during exposure to  $0.1 \frac{mg}{L}$  and decreased reads during exposure to  $3.0 \frac{mg}{L}$ . The genus *Cryomorpha*, a member of known organophosphate-degrading order Flavobacteriales, was associated with increased reads after 30 days exposure to malathion at  $0.1 \frac{mg}{L}$ .

## Bibliography

1. A. K. Janeczko, E. B. Walters, S. J. Schuldt, M. L. Magnuson, S. A. Willison, L. M. Brown, O. N. Ruiz, D. L. Felker, and L. Racz, "Fate of malathion and a phosphonic acid in activated sludge with varying solids retention times," *Water research* **57**, pp. 127–139, 2014.
2. G. Hamer, "Microbial consortia for multiple pollutant biodegradation," *Pure and Applied Chemistry* **69**(11), pp. 2343–2356, 1997.
3. B.-M. Wiln, B. Jin, and P. Lant, "Impacts of structural characteristics on activated sludge floc stability," *Water Research* **37**(15), pp. 3632–3645, 2003.
4. R. C. Gupta, *Handbook of toxicology of chemical warfare agents*, Academic Press, 2009.
5. L. London, A. Flisher, C. Wesseling, D. Mergler, and H. Kromhout, "Suicide and exposure to organophosphate insecticides: Cause or effect?," *American Journal of Industrial Medicine* **47**(4), pp. 308–321, 2005.
6. E. Baker, M. Zack, J. Miles, L. Alderman, M. Warren, R. Dobbin, S. Miller, and W. Teeters, "Epidemic malathion poisoning in pakistan malaria workers," *The Lancet* **311**(8054), pp. 31–34, 1978.
7. U. S. E. P. Agency, "Reregistration Eligibility Decision (RED) for Malathion." [http://www.epa.gov/oppsrrd1/REDs/malathion%5C\\_red.pdf](http://www.epa.gov/oppsrrd1/REDs/malathion%5C_red.pdf), 2014.
8. N. P. I. Center, "Malathion Technical Fact Sheet." <http://www.npic.orst.edu/factsheets/malatech.pdf>, 2014.
9. L. G. Costa, "Current issues in organophosphate toxicology," *Clinica chimica acta* **366**(1), pp. 1–13, 2006.
10. A. N. Bigley and F. M. Raushel, "Catalytic mechanisms for phosphotriesterases," *Biochimica et Biophysica Acta (BBA) - Proteins and Proteomics* **1834**(1), pp. 443–453, 2013.
11. Y. Zheng, L. Long, Y. Fan, J. Gan, J. Fang, and W. Jin, "A review on the detoxification of organophosphorus compounds by microorganisms," *African Journal of Microbiology Research* **7**(20), pp. 2127–2134, 2013.
12. B. K. Singh and A. Walker, "Microbial degradation of organophosphorus compounds," *FEMS microbiology reviews* **30**(3), pp. 428–471, 2006.
13. F. C. Hoskin, J. E. Walker, W.-D. Dettbarn, and J. R. Wild, "Hydrolysis of tetriso by an enzyme derived from pseudomonas diminuta as a model for the detoxication of o-ethyl s-(2-diisopropylaminoethyl) methylphosphonothiolate (vx)," *Biochemical Pharmacology* **49**(5), pp. 711–715, 1995.

14. K. Lai, N. Stolowich, and J. Wild, "Characterization of p-s bond hydrolysis in organophosphorothioate pesticides by organophosphorus hydrolase," *Archives of Biochemistry and Biophysics* **318**(1), pp. 59–64, 1995.
15. T.-C. Cheng, S. Harvey, and A. Stroup, "Purification and properties of a highly active organophosphorus acid anhydrolase from *alteromonas undina*," *Applied and Environmental Microbiology* **59**(9), pp. 3138–3140, 1993.
16. H. Imran, K. M. Altaf, J.-G. Kim, and C. Duckjin-Gu, "Malathion degradation by *Pseudomonas* using activated sludge treatment system (Biosimulator)," *Biotechnology* **3**(1), pp. 82–89, 2004.
17. E. Kannapiran and J. Ravindran, "Dynamics and diversity of phosphate mineralizing bacteria in the coral reefs of gulf of mannar," *Journal of Basic Microbiology* **52**(1), pp. 91–98, 2011.
18. S. Andleeb and J. I. Qazi, "Assessment of detoxification of malathion by *Pseudomonas* isolates," *African Journal of Microbiology Research* **8**(11), pp. 1170–1177, 2014.
19. I. Y. Mostafa, I. M. I. Fakhr, M. R. E. Bahig, and Y. A. El-Zawahry, "Metabolism of organophosphorus insecticides," *Archiv für Mikrobiologie* **86**(3), pp. 221–224, 1972.
20. S. Xie, J. Liu, L. Li, and C. Qiao, "Biodegradation of malathion by *Acinetobacter johnsonii* MA19 and optimization of cometabolism substrates," *Journal of Environmental Sciences* **21**(1), pp. 76–82, 2009.
21. Y. Lei, A. Mulchandani, and W. Chen, "Improved Degradation of Organophosphorus Nerve Agents and p-Nitrophenol by *Pseudomonas putida* JS444 with Surface-Expressed Organophosphorus Hydrolase," *Biotechnology progress* **21**(3), pp. 678–681, 2005.
22. E. B. Mardis, "Next-Generation Sequencing Technologies." [http://www.genome.gov/Pages/Research/IntramuralResearch/DIRCalendar/CTGA2012/CTGA2012%5C\\_Lec06%5C\\_color.pdf](http://www.genome.gov/Pages/Research/IntramuralResearch/DIRCalendar/CTGA2012/CTGA2012%5C_Lec06%5C_color.pdf), 2012.
23. J. Patel, "16S rRNA gene sequencing for bacterial pathogen identification in the clinical laboratory," *Molecular Diagnosis* **6**(4), pp. 313–321, 2001.
24. J. M. Janda and S. L. Abbott, "16S rRNA gene sequencing for bacterial identification in the diagnostic laboratory: pluses, perils, and pitfalls," *Journal of clinical microbiology* **45**(9), pp. 2761–2764, 2007.
25. S. He, F. I. Bishop, and K. D. McMahon, "Bacterial Community and "Candidatus Accumulibacter" Population Dynamics in Laboratory-Scale Enhanced Biological Phosphorus Removal Reactors," *Applied and Environmental Microbiology* **76**(16), pp. 5479–5487, 2010.



26. U. S. E. P. Agency, *Method 9040C ph Electrometric Measurement*, 2004.
27. E. W. Rice and L. Bridgewater, *Standard methods for the examination of water and wastewater*, American Public Health Association, 2012.
28. M. L. Inc., “PowerSoil® DNA Isolation Kit.” <http://www.mobio.com/images/custom/file/protocol/12888.pdf>, 2014.
29. T. F. Scientific, “T042-Technical Bulletin NanoDrop™ Spectrophotometers, 260/280 and 260/230 Ratios.” <http://www.nanodrop.com/Library/T042-NanoDrop-Spectrophotometers-Nucleic-Acid-Purity-Ratios.pdf>, 2010.
30. T. F. Scientific, “NanoDrop™ 1000 Spectrophotometer V3.8 User’s Manual.” <http://www.nanodrop.com/Library/nd-1000-v3.8-users-manual-8%20x11.pdf>, 2011.
31. L. T. Inc., “Qubit® 2.0 Fluorometer User’s Guide.” <http://www.lifetechnologies.com/content/dam/LifeTech/migration/en/filelibrary/cell-tissue-analysis/qubit-all-file-types.par.0519.file.dat/qubit-2-fluorometer-user-manual.pdf>, 2010.
32. R. Brankatschk, N. Bodenhausen, J. Zeyer, and H. Burgmann, “Simple Absolute Quantification Method Correcting for Quantitative PCR Efficiency Variations for Microbial Community Samples,” *Applied and Environmental Microbiology* **78**(12), pp. 4481–4489, 2012.
33. S. J. Flynn, F. E. Lffler, and J. M. Tiedje, “Microbial Community Changes Associated with a Shift from Reductive Dechlorination of PCE to Reductive Dechlorination of cis -DCE and VC,” *Environmental Science and Technology* **34**(6), pp. 1056–1061, 2000.
34. A. Klindworth, E. Pruesse, T. Schweer, J. Peplies, C. Quast, M. Horn, and F. O. Glockner, “Evaluation of general 16S ribosomal RNA gene PCR primers for classical and next-generation sequencing-based diversity studies,” *Nucleic Acids Research* **41**(1), pp. e1–e1, 2012.
35. I. Lopez, F. Ruiz-Larrea, L. Cocolin, E. Orr, T. Phister, M. Marshall, J. VanderGheynst, and D. A. Mills, “Design and Evaluation of PCR Primers for Analysis of Bacterial Populations in Wine by Denaturing Gradient Gel Electrophoresis,” *Applied and Environmental Microbiology* **69**(11), pp. 6801–6807, 2003.
36. J. R. de la Torre, B. M. Goebel, E. I. Friedmann, and N. R. Pace, “Microbial Diversity of Cryptoendolithic Communities from the McMurdo Dry Valleys, Antarctica,” *Applied and Environmental Microbiology* **69**(7), pp. 3858–3867, 2003.
37. S. Altschul, “Gapped BLAST and PSI-BLAST: a new generation of protein database search programs,” *Nucleic Acids Research* **25**(17), pp. 3389–3402, 1997.

38. C. Quast, E. Pruesse, P. Yilmaz, J. Gerken, T. Schweer, P. Yarza, J. Peplies, and F. O. Glockner, "The SILVA ribosomal RNA gene database project: improved data processing and web-based tools," *Nucleic Acids Research* **41**(D1), pp. D590–D596, 2012.
39. IDT, "OligoAnalyzer<sup>®</sup> program." <http://www.idtdna.com/Scitools>, 2014.
40. L. T. Inc., "Ion 16S<sup>™</sup> Metagenomics Kit." [https://tools.lifetechnologies.com/content/sfs/manuals/MAN0010799\\_Ion\\_16S\\_Metagenomics\\_UG.pdf](https://tools.lifetechnologies.com/content/sfs/manuals/MAN0010799_Ion_16S_Metagenomics_UG.pdf), 2014.
41. L. T. Inc., "Prepare Amplicon Libraries without Fragmentation Using the Ion Plus Fragment Library Kit." [http://ioncommunity.lifetechnologies.com/servlet/JiveServlet/downloadBody/3322-102-6-22243/MAN0006846%5C\\_RevA%5C\\_UB%5C\\_3March2014.pdf](http://ioncommunity.lifetechnologies.com/servlet/JiveServlet/downloadBody/3322-102-6-22243/MAN0006846%5C_RevA%5C_UB%5C_3March2014.pdf), 2014.
42. S. S. Inc, "Quick Guide CSD2010 Marker B." <http://www.sagescience.com/wp-content/uploads/2011/10/Quick-Guide-CSD2010-marker-B.pdf>, 2014.
43. A. T. Inc, "Agilent 2100 Bioanalyzer 2100 Expert User's Guide." [http://www.chem.agilent.com/library/usermanuals/Public/G2946-90004%5C\\_Vespucchi%5C\\_UG%5C\\_eBook%5C\\_\(NoSecPack\).pdf](http://www.chem.agilent.com/library/usermanuals/Public/G2946-90004%5C_Vespucchi%5C_UG%5C_eBook%5C_(NoSecPack).pdf), 2014.
44. L. T. Inc., "Ion PGM<sup>™</sup> Template OT2 400 Kit." [http://ioncommunity.lifetechnologies.com/servlet/JiveServlet/downloadBody/9110-102-2-23792/MAN0007219%5C\\_RevA%5C\\_QR%5C\\_15Sept2014.pdf](http://ioncommunity.lifetechnologies.com/servlet/JiveServlet/downloadBody/9110-102-2-23792/MAN0007219%5C_RevA%5C_QR%5C_15Sept2014.pdf), 2014.
45. H. Li, B. Handsaker, A. Wysoker, T. Fennell, J. Ruan, N. Homer, G. Marth, G. Abecasis, and R. Durbin, "The sequence alignment/map format and samtools," *Bioinformatics* **25**(16), pp. 2078–2079, 2009.
46. M. Martin, "Cutadapt removes adapter sequences from high-throughput sequencing reads," *EMBnet.journal* **17**, pp. 10–12, May 2011.
47. B. Chevreux, T. Wetter, and S. Suhai, "Genome sequence assembly using trace signals and additional sequence information," in *German Conference on Bioinformatics*, pp. 45–56, 1999.
48. D. H. Huson, S. Mitra, H.-J. Ruscheweyh, N. Weber, and S. C. Schuster, "Integrative analysis of environmental sequences using megan4," *Genome Research* **21**(9), pp. 1552–1560, 2011.
49. J. C. Wooley, A. Godzik, and I. Friedberg, "A primer on metagenomics," *PLoS Computational Biology* **6**(2), p. e1000667, 2010.
50. J. Fukuyama, P. Mcmurdie, L. Dethlefsen, D. Relman, and S. Holmes, *Comparisons of distance methods for combining covariates and abundances in micro biome studies*, pp. 3–4. Stanford University, 2012.

51. C. Kragelund, J. L. Nielsen, T. R. Thomsen, and P. H. Nielsen, "Ecophysiology of the filamentous alphaproteobacterium meganema perideroedes in activated sludge," *FEMS Microbiology Ecology* **54**(1), pp. 111–112, 2005.
52. M. Dworkin and S. Falkow, *The Prokaryotes: Vol. 7: Proteobacteria: Delta and Epsilon Subclasses. Deeply Rooting Bacteria*, The Prokaryotes, Springer, 2006.
53. Y. Davidov, "Diversity and evolution of bdellovibrio-and-like organisms (balos), reclassification of bacteriovorax starrii as peredibacter starrii gen. nov., comb. nov., and description of the bacteriovorax-peredibacter clade as bacteriovoracaceae fam. nov.," *International Journal of Systematic and Evolutionary Microbiology* **54**(5), pp. 1439–1452, 2004.
54. J. M. Macy, S. Rech, G. Auling, M. Dorsch, E. Stackebrandt, and L. I. Sly, "Thauera selenatis gen. nov., sp. nov., a member of the beta subclass of proteobacteria with a novel type of anaerobic respiration," *International Journal of Systematic Bacteriology* **43**(1), pp. 135–142, 1993.
55. B. Song, N. Palleroni, L. Kerkhof, and M. Hggblom, "Characterization of halobenzoate-degrading, denitrifying azoarcus and thauera isolates and description of thauera chlorobenzoica sp. nov.," *International Journal of Systematic and Evolutionary Microbiology* **51**(2), pp. 589–602, 2001.
56. A. M. Maszenan, R. J. Seviour, B. K. C. Patel, G. N. Rees, and B. M. McDougall, "Amaricoccus gen. nov., a gram-negative coccus occurring in regular packages or tetrads, isolated from activated sludge biomass, and descriptions of amaricoccus veronensis sp. nov., amaricoccus tamworthensis sp. nov., amaricoccus macauensis sp. nov., and amaricoccus kaplicensis sp. nov.," *International Journal of Systematic Bacteriology* **47**(3), pp. 727–734, 1997.
57. V. L. Y. J D Rihs, "Roseomonas, a new genus associated with bacteremia and other human infections.," *Journal of Clinical Microbiology* **31**(12), p. 3275, 1993.
58. D. Kirchman, "The ecology of cytophaga flavobacteria in aquatic environments," *FEMS Microbiology Ecology* **39**(2), pp. 91–100, 2002.
59. L. I. Sly, M. Taghaviti, and M. Fegan, "Phylogenetic heterogeneity within the genus herpetosiphon: transfer of the marine species herpetosiphon cohaerens, herpetosiphon nigricans and herpetosiphon persicus to the genus lewinella gen. nov. in the flexibacter-bacteroides-cytophaga phylum," *International Journal of Systematic Bacteriology* **48**(3), pp. 731–737, 1998.
60. J. P. Bowman, "Algoriphagus ratkowskyi gen. nov., sp. nov., brumimicrobium glaciale gen. nov., sp. nov., cryomorpha ignava gen. nov., sp. nov. and crocinitomix catalasitica gen. nov., sp. nov., novel flavobacteria isolated from various polar habitats," *International Journal of Systematic and Evolutionary Microbiology* **53**(5), pp. 1343–1355, 2003.

61. T. Hofstad, I. Olsen, E. R. Eribe, E. Falsen, M. D. Collins, and P. A. Lawson, "Dysgonomonas gen. nov. to accommodate dysgonomonas gadei sp. nov., an organism isolated from a human gall bladder, and dysgonomonas capnocytophagoides (formerly cdc group df-3)," *International Journal of Systematic and Evolutionary Microbiology* **50**(6), pp. 2189–2195, 2000.
62. Y.-H. Zhang, D. Xu, J.-Q. Liu, and X.-H. Zhao, "Enhanced degradation of five organophosphorus pesticides in skimmed milk by lactic acid bacteria and its potential relationship with phosphatase production," *Food Chemistry* **164**(0), pp. 173 – 178, 2014.
63. I. S. Kulichevskaya, N. E. Suzina, W. Liesack, and S. N. Dedysh, "Bryobacter aggregatus gen. nov., sp. nov., a peat-inhabiting, aerobic chemo-organotroph from subdivision 3 of the acidobacteria," *International Journal of Systematic and Evolutionary Microbiology* **60**(2), pp. 301–306, 2009.
64. Y. Sekiguchi, "Anaerolinea thermophila gen. nov., sp. nov. and caldilinea aerophila gen. nov., sp. nov., novel filamentous thermophiles that represent a previously uncultured lineage of the domain bacteria at the subphylum level," *International Journal of Systematic and Evolutionary Microbiology* **53**(6), pp. 1843–1851, 2003.
65. A. McGuire, B. Weiner, S. Park, I. Wapinski, S. Raman, G. Dolganov, M. Peterson, R. Riley, J. Zucker, and T. e. a. Abeel, "Comparative analysis of mycobacterium and related actinomycetes yields insight into the evolution of mycobacterium tuberculosis pathogenesis," *BMC Genomics* **13**(1), p. 120, 2012.
66. A. McGuire, B. Weiner, S. Park, I. Wapinski, S. Raman, G. Dolganov, M. Peterson, R. Riley, J. Zucker, and T. e. a. Abeel, "Comparative analysis of mycobacterium and related actinomycetes yields insight into the evolution of mycobacterium tuberculosis pathogenesis," *BMC Genomics* **13**(1), p. 120, 2012.

# REPORT DOCUMENTATION PAGE

Form Approved  
OMB No. 0704-0188

The public reporting burden for this collection of information is estimated to average 1 hour per response, including the time for reviewing instructions, searching existing data sources, gathering and maintaining the data needed, and completing and reviewing the collection of information. Send comments regarding this burden estimate or any other aspect of this collection of information, including suggestions for reducing this burden to Department of Defense, Washington Headquarters Services, Directorate for Information Operations and Reports (0704-0188), 1215 Jefferson Davis Highway, Suite 1204, Arlington, VA 22202-4302. Respondents should be aware that notwithstanding any other provision of law, no person shall be subject to any penalty for failing to comply with a collection of information if it does not display a currently valid OMB control number. **PLEASE DO NOT RETURN YOUR FORM TO THE ABOVE ADDRESS.**

<b>1. REPORT DATE (DD-MM-YYYY)</b> 26-03-2015			<b>2. REPORT TYPE</b> Master's Thesis		<b>3. DATES COVERED (From — To)</b> Sep 2013 - Mar 2015	
<b>4. TITLE AND SUBTITLE</b>  Effect of Malathion on the Microbial Ecology of Activated Sludge					<b>5a. CONTRACT NUMBER</b>	
					<b>5b. GRANT NUMBER</b>	
					<b>5c. PROGRAM ELEMENT NUMBER</b>	
<b>6. AUTHOR(S)</b>  Martin, Seth K., SMSgt, USAF					<b>5d. PROJECT NUMBER</b>  15V115A	
					<b>5e. TASK NUMBER</b>	
					<b>5f. WORK UNIT NUMBER</b>	
<b>7. PERFORMING ORGANIZATION NAME(S) AND ADDRESS(ES)</b> Air Force Institute of Technology Graduate School of Engineering and Management 2950 Hobson Way, Building 640 WPAFB OH 45433-7765					<b>8. PERFORMING ORGANIZATION REPORT NUMBER</b>  AFIT-ENV-MS-15-M-095	
<b>9. SPONSORING / MONITORING AGENCY NAME(S) AND ADDRESS(ES)</b> Environmental Protection Agency National Homeland Security Research Center 26 West Martin Luther King Drive Cincinnati, OH 45268 Matthew Magnuson 513-569-7321, magnuson.matthew@epa.gov					<b>10. SPONSOR/MONITOR'S ACRONYM(S)</b>  EPA/NHSRC	
					<b>11. SPONSOR/MONITOR'S REPORT NUMBER(S)</b>	
<b>12. DISTRIBUTION / AVAILABILITY STATEMENT</b>  DISTRIBUTION STATEMENT A. APPROVED FOR PUBLIC RELEASE; DISTRIBUTION IS UNLIMITED.						
<b>13. SUPPLEMENTARY NOTES</b>  "This work is declared a work of the U.S. Government and is not subject to copyright protection in the United States."						
<b>14. ABSTRACT</b> Decontamination activities may cause the release of contaminated washwater into the wastewater that eventually flows into a wastewater treatment facility. This raises concerns about the effect of chemical warfare agents (CWAs) on the microbial consortia that are responsible for cleaning the wastewater. This study investigated the impact of malathion on the microbial ecology of laboratory scale activated sludge communities. The Simpson Reciprocal Index decreased for three bioreactors operated in the absence of malathion, which showed that the microbial assemblage became less diverse during the course of the study. The species identified in the bioreactors belonged to well-known groups of heterotrophic and autotrophic bacteria, and these groups were represented in the presence and absence of malathion. Nitrospira, a key player in autotrophic nitrogen removal, decreased in relative abundance for the bioreactor exposed to 0.1 mg/L of malathion but increased in the bioreactor exposed to 3 mg/L of malathion, possibly due to interactions with heterotrophic groups that suffered inhibition. To the author's knowledge, this study is the first to document the ecological impacts of long term malathion exposure in bioreactors carrying out COD removal and nitrification.						
<b>15. SUBJECT TERMS</b>  Activated Sludge, Organophosphates, Wastewater Treatment, Sequencing, Bacteria						
<b>16. SECURITY CLASSIFICATION OF:</b>			<b>17. LIMITATION OF ABSTRACT</b>	<b>18. NUMBER OF PAGES</b>	<b>19a. NAME OF RESPONSIBLE PERSON</b>	
<b>a. REPORT</b>	<b>b. ABSTRACT</b>	<b>c. THIS PAGE</b>			Dr. Willie F. Harper, AFIT/ENV	
U	U	U	UU	77	<b>19b. TELEPHONE NUMBER (include area code)</b> (937) 255-3636 ext 4528; willie.harper@afit.edu	